Inorganic Chemistry

pubs.acs.org/IC

Article

Synergy Effects in Heavy Metal Ion Chelation with Aryl- and Aroyl-Substituted Thiourea Derivatives

Ransel Barzaga, Lucia Lestón-Sánchez, Fernando Aguilar-Galindo, Osvaldo Estévez-Hernández, and Sergio Díaz-Tendero*

Cite This: *Inorg. Chem.* 2021, 60, 11984−12000

Read Online

ACCESS | Metrics & More | Article Recommendations | Supporting Information

ABSTRACT: Detection and removal of metal ion contaminants have attracted great interest due to the health risks that they represent for humans and wildlife. Among the proposed compounds developed for these purposes, thiourea derivatives have been shown as quite efficient chelating agents of metal cations and have been proposed for heavy metal ion removal and for components of high-selectivity sensors. Understanding the nature of metal−ionophore activity for these compounds is thus of high relevance. We present a theoretical study on the interaction between substituted thioureas and metal cations, namely, Cd^{2+}, Hg^{2+}, and Pb^{2+}. Two substituent groups have been chosen: 2-furoyl and *m*-trifluoromethylphenyl. Combining density functional theory simulations with wave function analysis techniques, we study the nature of the metal−thiourea interaction and characterize the bonding properties. Here, it is shown how the *N*,*N*′-disubstituted derivative has a strong affinity for Hg^{2+}, through cation−hydrogen interactions, due to its greater oxidizing capacity.

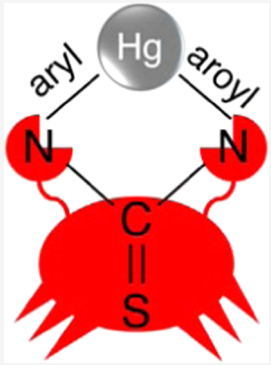

INTRODUCTION

Among the most toxic environmental pollutants are heavy metals.[1−3] In addition to their toxicity, their persistence in the environment, since they are non-biodegradable; their tendency to biomagnificate; and their bioaccumulative nature make them contaminants whose detection and removal are essential.[4−7] Several kinds of heavy metal-detection sensors have been developed,[8] such as biosensors,[9−13] electrochemical sensors,[14−18] nanomaterial-based sensors,[19−22] and optical sensors.[23−25] Today, intense research activity is focused on increasing both the sensitivity and selectivity in detection by these devices.[26−31] In this way, thiourea derivatives have been developed as a new type of organic ionophores for heavy metal ion selective electrodes.[32,33] One of the processes to eradicate such pollutants is chemical remediation, which consists of the complexation of the ions using chelating ligands.[34−38] Thiourea derivatives are promising chelating agents of metal cations that have also been proposed for heavy metal ion removal.[39−51] Both for sensing and for removal reasons, understanding heavy metal−ionophore activity by organic compounds is thus of high relevance.[52−54] In this context, several studies have focused on metal complexes with thiourea derivatives. Coordination chemistry of alkyl and acyl(aroyl) thioureas of Pt(II), Pd(II), and Rh(III) was reviewed by Koch;[55] the chemistry and metal complexes of acyl-thiourea compounds were recently reviewed in ref 56 ; and uranyl complexes have also been reported with thiourea derivatives.[57]

Quantum chemistry emerges as a reliable tool to predict ionophore properties of organic compounds. Indeed, the investigation of interactions between metallic cations and organic compounds has attracted huge interest in the last few decades, where an important activity has been developed by means of computational chemistry.[58−75] In many studies, the theory has been combined with experiments, typically carried out with mass spectrometry techniques.[76−97] The nature of the metal ion−molecule interaction, the reactivity of the new compounds, and the change in structural and spectroscopic properties of the organic molecules upon ion complexation are among the most important aspects investigated in these studies.

We present here a theoretical study on the interaction between substituted thioureas and three heavy metal ions, namely, Cd^{2+}, Hg^{2+}, and Pb^{2+}, all of them well-known pollutants. First, we focus on the interactions of these cations with the canonical thiourea, mainly characterizing the metal−sulfur and metal−nitrogen bonds. In this part of the study, we have also performed molecular dynamics simulations allowing us to evaluate the evolution of the complexes over time. Among the different identified channels, Coulomb explosion is dominant for Hg^{2+} complexes. In the second part, we study mono- and *N*,*N*′-disubstituted thioureas. We have chosen as substituents 2-furoyl and *m*-trifluoromethylphenyl, inspired by the studies of Otazo-Sánchez and collaborators.[32,33] These

Received: April 7, 2021
Published: July 26, 2021

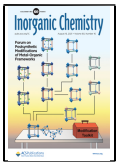

https://doi.org/10.1021/acs.inorgchem.1c01068
Inorg. Chem. 2021, 60, 11984−12000

studies evaluate the stereoelectronic factors that can influence the nucleophilicity of the sulfur atom as the main coordination center of thiourea derivatives in the search for the best ionophores for the development of selective electrodes to detect pollutant metal ions, such as Pb(II), Cd(II), and Hg(II). These studies point out *N*-(2-furoyl) and *N*-(*m*-trifluoromethylphenyl)thiourea derivatives as good candidates. In ref 33, the intramolecular hydrogen bond in *N*,*N*′-disubstituted acyl thioureas is confirmed, suggesting an enhancement in the metal affinity of these compounds. These substituents are Lewis bases with lone pair electrons available to interact with the metal cation; different binding sites in each substituent can act independently or in a coordinated way linking the metal. The aim of the study is to understand the nature of such interactions and to evaluate the effect of the substituents. To do this, we first evaluate the interaction between the ions and the bare thiourea, then with just one of the substituents, and finally with both of them. We also study the effect of the heavy metal ion interaction in the thioketone−thioenol tautomerism. The different behavior in the bonding properties of each ion points toward the selectivity of the proposed derivatives, in particular, due to the cooperative effect when both substituents are present.

COMPUTATIONAL DETAILS

All electronic structure calculations have been performed in the framework of the density functional theory (DFT) using the Gaussian09 package.[98] In particular, we have employed the well-known B3LYP hybrid functional[99,100] with the all-electron 6-31++G(d,p) Pople's double-zeta basis set[101] for nonmetallic atoms (H, C, N, O, F, and S) and the valence+pseudo SDD basis set[102] for the metallic centers (Pb, Cd, or Hg). The use of pseudopotentials allows us to minimize the computational effort by a reduction of the explicit number of electrons in the calculation. Under this approach, we can correctly describe the effect of the core electrons in the valence states without performing relativistic corrections that might be important for heavy atoms. All stationary points have been proved to be minima in the potential energy surface (PES) through the calculation of the second derivatives. To obtain a wide set of isomers, we have performed a conformational analysis constraining the rotation around specific dihedral angles. Accordingly, the N−C−N−H angles have been selected for all compounds. Although in the case of the *N*-monosubstituted and *N*,*N*′-disubstituted derivatives, the H−N−R_C−X angles have also been added, where X = R_C or R_O which represent the C and O atoms in the functional group, respectively.

Molecular dynamics (MD) simulations were performed with the atom-centered density matrix propagation (ADMP),[103−105] imposing a full self-consistent calculation in each propagation step (*FullSCF* option in Gaussian09), thus ensuring adiabaticity along the simulation (t_{max} = 1 ps with a time step of Δt = 0.1 fs). We have computed 100 trajectories starting from the most stable minimum of each thiourea−metal complex and with internal excitation energy (kinetic energy of the nuclei) equal to the difference between the energy of the initial structure and the thiourea + M^{2+} at infinite distance. This energy was initially randomly distributed between all nuclear degrees of freedom of the system.

To obtain further insights into the electronic structure and the bonding of the thiourea−metal complexes, we performed an exhaustive analysis using the quantum theory of atoms in molecules (QTAIM).[106] To do this, we used the AimAll software.[107]

The Gibbs free energy for the complexation reaction

$$\text{cation} + \text{molecule} \rightarrow \text{complex} \quad (1)$$

has been computed as

$$\Delta G = G_{complex} - (G_{cation} + G_{molecule}) \quad (2)$$

where G_i is the Gibbs free energy of the molecule, complex, or cation. We use as $G_{molecule}$ the Gibbs free energy of the thione or thiol form of the molecule to which the cation binds.

RESULTS AND DISCUSSION

In this section, we analyze the interaction between Cd(II), Hg(II), Pb(II) and the canonical (**1**), *N*-monosubstituted (**2**, **3**), and *N*,*N*′-disubstituted (**4**) thiourea structures. The results are systematically presented in the corresponding subsections. In each subsection, we first present the study of the free molecule focusing on its tautomerization equilibrium. Subsequently, the cation−molecule interaction is discussed for the most stable conformations and tautomers in each case by means of energetic parameters and wave function analysis. In the particular case of cation−thiourea systems, a molecular dynamics study is also included. In the following, the tautomers are distinguished from their isomers by a superscript index; e.g., structure **1a** is the canonical thione form of the thiourea and **1a**' is the thiol form. In the case of the complexes, the labeling of structures follows the same idea: thione and thiol forms are separately indicated in parentheses with a number for each complex; e.g., structure **9**(**1a**) corresponds to Hg(II) interacting with the thione form of **1a** and **19**'(**1a**') is a complex formed by Pb(II) and the thiol form of **1a**'. Each tautomerization equilibrium is described with a double arrow, the smallest one pointing to the less stable structure. Consequently, Gibbs free energies in these equilibria are always given with respect to the less stable reaction, therefore remaining a positive value. On the other hand, Gibbs free energies of complex formation are negative values due to the metal−thiourea interaction. Further information on the cation−molecule complexes is presented in the Supporting Information.

Canonical Thiourea. The canonical thiourea is characterized by a thione−thiol tautomeric equilibrium (see Scheme 1), which results in proton migration and the formation of a double C=N bond.[108−110] The thione conformation, **1a**, of thiourea is the most stable form, as can be seen from the Gibbs free energy difference. This equilibrium is displaced in favor of **1a** by 54.58 kJ·mol^{-1}, which is in close agreement with previous theoretical predictions at the MP2 level.[111] More

Scheme 1. Thione−Thiol Tautomeric Equilibrium of Thiourea[a]

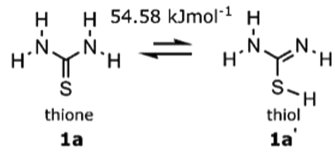

[a]Small and large arrows represent the unfavorable and favorable reactions, respectively. Relative Gibbs free energy between both forms is given in kJ·mol^{-1}; notice that it does not correspond to the taumerization barrier.

https://doi.org/10.1021/acs.inorgchem.1c01068
Inorg. Chem. 2021, 60, 11984−12000

conformers of the thione and thiol forms are depicted in the Supporting Information.

To explore the interaction of the cations with **1a** and **1a′**, several initial spatial configurations were considered by placing them at the nucleophilic centers: nitrogen and sulfur atoms (see all obtained geometries in the Supporting Information and the most relevant ones in Scheme 2). The DFT-optimized

Scheme 2. All of the Cation−Molecule Interactions Observed after Geometry Optimization[a]

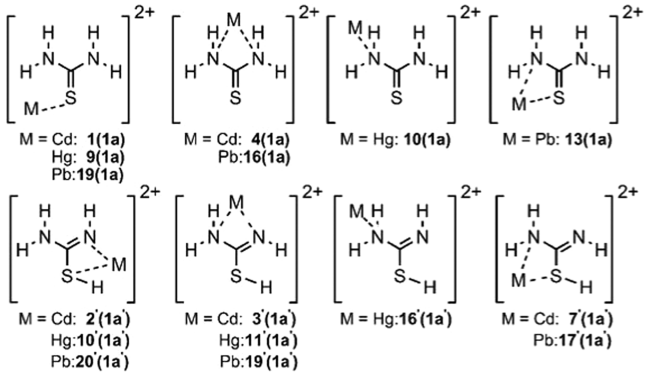

[a]A "ball-and-stick" model of these structures is given in Figures 1 and S2.

complexes can exhibit a monodentate character with the metal cation linked through the sulfur atom (M−S) or to the nitrogen atom (M−N) or a bidentate interaction (N−M−N or S−M−N). Examples of monodentate interaction with nitrogen are structures **10**(**1a**) or **16′**(**1a′**); with the sulfur atom, **1**(**1a**) or **9**(**1a**); bidentate, N−M−S **2′**(**1a′**) or **10′**(**1a′**); and bidentate N−M−N **3′**(**1a′**) or **19′**(**1a′**).

Although the cation can bind through different nucleophilic centers, the most stable interaction is the S-monodentate structures for the three metal cations: **1**(**1a**), **9**(**1a**), and **19**(**1a**) for Cd(II), Hg(II), and Pb(II), respectively (see Scheme 2). A similar trend has been observed in the reaction between thiourea and other divalent cations, such as Ca(II), Cu(II), and Zn(II).[83,112,113] In these complexes, the geometry does not suffer strong deformations; only some elongation of the C=S bond due to a charge transferred from the $\pi_{C=S}$ orbital toward the new metal−S bond. However, in those complexes where the metal cation binds to nitrogen atoms, either N−M monodentate or N−M−N/S−M−N bidentate, much more marked changes in the geometry are observed upon complexation (see Figure 1). The geometry shows that the N atoms involved in the interaction present a tetrahedral-sp^3 chemical environment. This is a clear indication of the cation−molecule interaction, which modifies the original planar-sp^2 bonding of NH_2.

Table 1 shows Gibbs free energies of formation for all S-monodentate complexes in their thione or thiol forms. According to these values, the formation of the complexes is more favored for the thione form of the thiourea. Furthermore, it can also be observed that the complexation energy decreases in the order Hg(II) > Cd(II) > Pb(II) for both forms, indicating a trend in the chemical affinity of the cations. Interestingly, this chemoselectivity for Hg(II) makes more stable its thiol S−M−N bidentate complex (747.9 kJ·mol^{-1}) than the thione S-monodentate complex with Pb(II) and

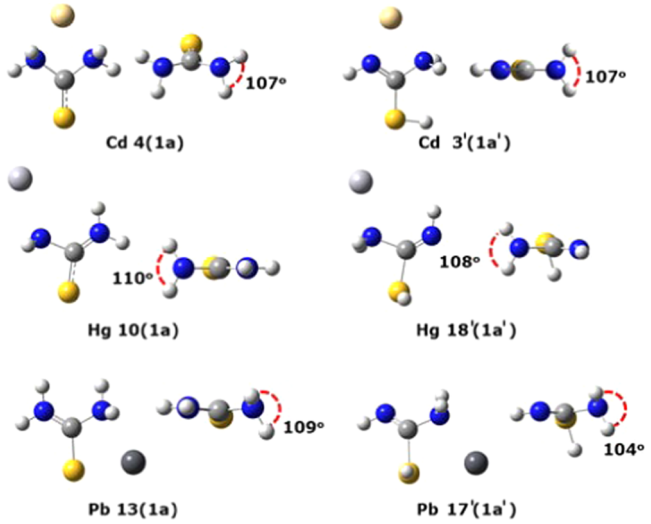

Figure 1. DFT-optimized structures of the N-monodentate and N−N and S−N−bidentate complexes. The NH_2 bonding angle is highlighted with a red dashed line. In the top view, the cation has been omitted for better visualization.

Table 1. Gibbs Free Energy of Formation (Δ*G*) and Cation Charge (*q*) for the Thione (1a) and Thiol (1a′) Forms of the Cation−Molecule Complexes

	thione			thiol	
	Δ*G* (kJ·mol^{-1})	*q* (e^-)		Δ*G* (kJ·mol^{-1})	*q* (e^-)
Cd 1(**1a**)	−669.8	1.13	**Cd 2′**(**1a′**)	−643.8	1.33
Hg 9(**1a**)	−826.6	0.91	**Hg 10′**(**1a′**)	−747.9	1.15
Pb 19(**1a**)	−459.5	1.39	**Pb 20′**(**1a′**)	−473.6	1.48

Cd(II) (459.5 and 669.9 kJ·mol^{-1}, respectively); see structures **10′**(**1a′**), **1**(**1a**), and **19**(**1a**) in Scheme 2.

As can be seen in Table 1, none of the cations retain the positive divalent charge (*q*) after complex formation, an indication of the cation−molecule charge transfer. All of the cations act as oxidant agents, attracting electron density from the molecule. The highest positive charge is observed for Pb(II) while for Hg(II), it decreases considerably. The highest oxidation character shown by Hg(II) can be explained by the polarizability of this cation, which allows for a stronger electron cloud deformation, easing the accommodation of the charge transferred from the molecule.

The chemical nature of the cation−molecule interaction has been studied from a topological analysis of the electron density distribution. To do this, several properties at the most relevant bond critical points (BCPs) in the cation−molecule complexes were studied: (i) the total electron density (ρ); (ii) the Laplacian of the electron density ($\nabla^2\rho$), which is used to distinguish between closed shell (CS) interactions if this magnitude is positive or shared shell (SS) if it is negative; and (iii) the kinetic (*G*), potential (*V*), and total ($H = G + V$) energy density. The potential energy density *V* is always negative and gives the contribution of the covalent character to the interaction; the kinetic energy density *G* is always positive and provides the contribution of the ionic character. The sum of both gives the total electronic energy density *H*, and hence, one can easily predict the character of the interaction with the sign of H in the BCP: $H < 0$ is an indication of covalent with SS interactions and on the contrary, $H > 0$ reflects the ionic

https://doi.org/10.1021/acs.inorgchem.1c01068
Inorg. Chem. 2021, 60, 11984−12000

character of the bond with CS type of interactions.[114] Due to the mixed effects of valence shells acting in the cation−molecule interactions studied here, the full bond chemical nature is not always attained from a straightforward comparison of these properties (ρ, $\nabla^2\rho$, and H). Thus, a better description can be obtained with the ratio $|V|/G$, which allows for the classification of pure *CS* interactions ($|V|/G < 1$) or pure *SS* interactions ($|V|/G > 2$), as well as the intermediate region between them;[115,116] thus, a value of $|V|/G$ close to 2 is an indication of a covalent bond, and close to 1 of an ionic bond.

In Figure 2, we show the BCPs (green points) for the complexes of Cd(II) interacting with the thione and thiol

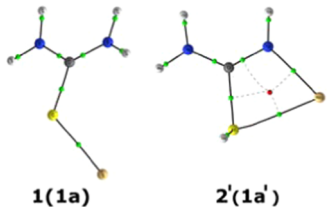

Figure 2. Representation of the cation−molecule BCPs, in green, for the most stable Cd−molecule complexes. Due to structural resemblance, the Pb and Hg complexes have been omitted. The bond length and the atomic radius have been resized for better visualization of the BCPs. In addition, the ring critical point in the thiol form (**2′**(**1a′**)) is represented in red.

Table 2. Electron Density Properties at the BCPs of Interest in the Cation−Molecule Complexes

	BCP	ρ (a.u.)	r (Å)	$\nabla^2\rho$ (a.u.)	H (a.u.)	$\|V\|/G$
1a	C−S	0.212	1.675	0.003	−0.249	
Cd 1(**1a**)	C−S	0.186	1.805	−0.330	−0.139	
	Cd−S	0.068	2.443	0.122	−0.016	1.339
Hg 9(**1a**)	C−S	0.185	1.810	−0.329	−0.136	
	Hg−S	0.076	2.442	0.108	−0.019	1.415
Pb 19(**1a**)	C−S	0.187	1.793	−0.337	−0.145	
	Pb−S	0.066	2.599	0.120	−0.017	1.898
1a′	C−S	0.190	1.799	−0.348	−0.139	
Cd 2′(**1a′**)	C−S	0.179	1.842	−0.301	−0.121	
	Cd−S	0.041	2.721	0.094	−0.005	1.182
	Cd−N	0.084	2.141	0.345	−0.013	1.128
Hg 10′(**1a′**)	C−S	0.182	1.831	−0.317	−0.128	
	Hg−S	0.037	2.847	0.087	−0.003	1.119
	Hg−N	0.095	2.150	0.319	−0.021	1.208
Pb 20′(**1a′**)	C−S	0.184	1.824	−0.325	−0.130	
	Pb−S	0.030	3.013	0.060	−0.003	1.319
	Pb−N	0.078	2.303	0.262	−0.014	1.453

forms as an example, and Table 2 summarizes the electron density properties at the BCPs involving the cation−molecule interactions for the most stable structures. A decrease of the electron density ρ at the C−S BCP is observed in all complexes with respect to the free molecules either in their thione or thiol forms (**1a**, **1a′**). Accordingly, a clear elongation of the C−S bond in the complexes is noted. These two features highlight the charge transfer process from the C=S bond of the molecule to the cation. Positive values of $\nabla^2\rho$ at the cation−S BCP illustrates the presence of CS interactions, which can be characterized as a combination of charge transfer and ion-induced dipole interactions. The smaller values of $\nabla^2\rho$ around the cation−S BCP for the thiol forms of the complexes (**2′**(**1a′**), **10′**(**1a′**), **20′**(**1a′**)) is a consequence of the electron-deficient C−S bond of **1a′**. On the contrary, the $\nabla^2\rho$ exhibited noticeable positive values at the cation−N BCP of the thiol complexes, evidence of the more electrostatic-type interactions in this case. However, for all complexes, we observe that $H < 0$ in the studied BCPs, which indicates a short degree of covalent cation−molecule interactions. The ratio $|V|/G$ in complexes with the thione form **1a** shows that the degree of covalency in Pb(II) is closer to a pure *SS* interaction ($|V|/G > 2$) than in Cd(II) and Hg(II). This is due to the valence shell of the cations: while Pb(II) has a $d^{10}s^2$ electronic configuration, for Cd(II) and Hg(II), it is d^{10}. Since overlapping of the atomic orbitals requires resemblance in symmetry and closeness in energy to build the covalent bonding, the s orbitals of Pb(II) present a higher overlapping with the lone pairs of the S atom than in the case of the d orbitals of Cd(II) and Hg(II). However, Pb(II) complexes present the lowest stabilization in the complexation process (according to the values in Table 1). This finding highlights the importance of the electrostatic and the ion-induced dipole kind of interactions, commonly present in cation−molecule complexes, on increasing the binding strength.[117−119]

To get a deeper insight into the stability of the complexes formed with thiourea, we have performed molecular dynamics (MD) simulations using the ADMP method (see the computational details). The initial geometry chosen for such simulations is the most stable structure found for each metal, i.e., **1**(**1a**) for Cd(II), **9**(**1a**) for Hg(II), and **19**(**1a**) for Pb(II). For each structure, we have performed 100 trajectories where the excitation energy is randomly redistributed into nuclear degrees of freedom; the excitation energy is the complexation energy in each case. At the end of the propagation time, we run statistics on the populated channels (see Figure 3). We consider that two molecular fragments have been formed when the distance between the atoms in each fragment is larger than 3.5 Å. No fragmentation is observed for the Pb(II) complex, and the only channel detected is formation of the complex. This is also observed as the main channel for Cd(II), although

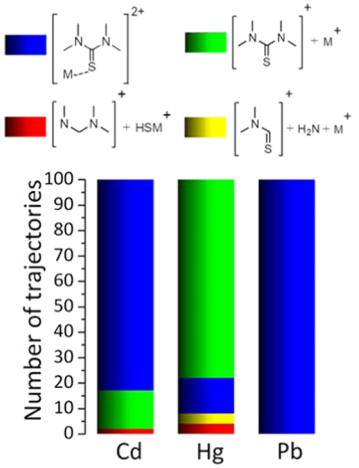

Figure 3. Identification of the channels observed during the MD simulation of cation−molecule complexes over the 100 trajectories considered. The fragmentation difference in different channels is highlighted.

https://doi.org/10.1021/acs.inorgchem.1c01068
Inorg. Chem. 2021, 60, 11984−12000

in this case, fragments of different species are also observed to a lesser extent. For Hg(II), fragmentation is predominant over complex formation: repulsion between the two positive charges leads to a dominant Coulomb explosion channel in $Hg^+ + \mathbf{1a}^+$. It can be followed by the release of neutral moieties from the cationic thiourea: $Hg^+ + NH_2 - C{=}S^+ + NH_2$. Similar Coulomb repulsion processes have been reported in previous theoretical studies that addressed the reaction between thiourea and Ca(II).[120]

We have further evaluated the cleavage time of the cation−molecule bonding for metals showing Coulomb explosion: Cd(II) and Hg(II). The goal is to clarify the stability and lifetime of such species before fragmentation occurs. For this purpose, we have analyzed trajectories that lead to a molecule−metal repulsion and have considered that the metal−S bond is broken when a distance greater than 3.0 Å is achieved for the first time in the trajectory; we assume that at longer distances, the system evolves toward dissociation since the charge is divided and both fragments repel each other. Then, the simulation time at which this event occurs is recorded (see the statistics in Figure 4). For Cd(II), bond weakening is a process

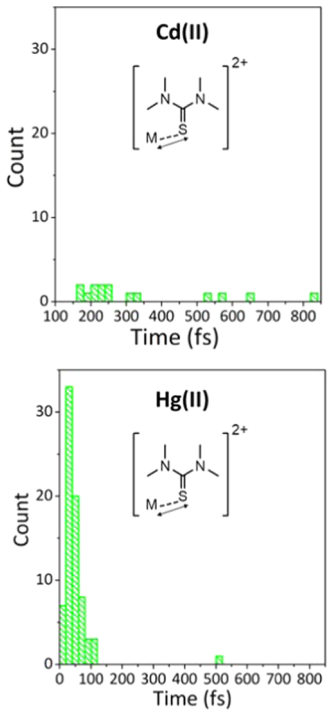

Figure 4. Counting of bond weakening events for the fragmentation channels of Cd(II) and Hg(II) describing the Coulomb explosion during the MD simulation.

that constitutes 15% of the total events within the MD propagation time. These events occur mainly in a time interval typically ranging from 150 to 350 fs, although above 500 fs some individual events are also observed. Bond weakening in Hg(II) represents 80% of the events and is a much faster process, taking place in the first 100 fs in most trajectories, a phenomenon that highlights the short time required to attain the Coulomb explosion between Hg(II) and the thiourea after complexation. The marked difference of Hg(II) with respect to the other cations may be related to the ease with which the charge transfer process occurs. Coulomb explosion requires that the metal atom and the molecule are positively charged, as well as that the corresponding repulsion forces overcome the bond formation energy.[121] Therefore, in Hg(II), the cause of Coulomb explosion can be explained by its higher ionization potential in comparison to Cd(II) and Pb(II):[122] Hg(II) shows higher preference than Cd(II) and Pb(II) to host electrons; consequently, charge transfer occurs in a lower time regime for Hg(II) provoking the ionization of the molecule to surpass bond formation. The relationship between the ionization potential of the cation and the occurrence of Coulomb explosion follows a trend that has been previously pointed out in other molecule−cation systems.[63,123,124] Other channels might occur at lower energy, but Coulomb explosion is dominant, mainly for Hg complexes, due to favorable entropic effects. The different behavior of Hg is also reflected in the monosubstituted and disubstituted thiourea complexes.

Effects of *N*-Monosubtitution. The functionalization of thiourea with the fragments 2-furoyl (structure **2**) and *m*-trifluoromethylphenyl (structure **3**) modifies some of the chemical properties previously discussed. First, hydrogen migration caused by the tautomeric equilibrium can occur in two different ways as can be seen in Scheme 3 (all computed structures can be found in the Supporting Information). Thiol forms can adopt different configurations depending on the hydrogen position and which nitrogen donates it.[125] Thiol tautomers with an amine group ($-NH_2$) have been labeled with a single superscript (**2a′**, **3a′**) and thiol forms with an unsaturated −NH group with a double superscript (**2a″**, **3a″**). Different letters have been used to distinguish when the tautomeric forms attain a structural change caused by isomerization (e.g., **2a″**, **2c″**). Positive Gibbs free energies allow us to recognize that the thione form (**2a** for 2-furoyl and **3a** for *m*-trifluoromethylphenyl) remains the most stable structure. Furthermore, the less stable form **2d** shows an energetic difference with respect to **2a′** below 5 $kJ{\cdot}mol^{-1}$. Such a difference between tautomers is not a considerable threshold and highlights the stability of thione forms[125−127] (see also Scheme 3, where relative energies between both forms in each equilibrium are given).

According to the results given in Scheme 3, for 2-furoyl thiourea, the thiol form **2a′** is more stable than **2a″**. This difference is a consequence of the structural changes during tautomerization that provoked **2a′** to exhibit a hyperconjugation effect from the C=N bond on the furan ring. Hyperconjugation is a well-known stabilizing interaction,[128−130] thereby explaining the energetic difference between **2a′** and **2a″**. Further stabilization of **2a′** occurs when it is isomerized to **2c′**. The appearance in **2c′** of SH···O hydrogen bonding enhances the hyperconjugation effect and simultaneously increases the structural stability.[131−134] Evidence of the effect of SH···O bonding is also noticeable in the equilibrium **2a″** → **2d″**. Notice also in Scheme 3 that the cis-trans conformers **2a″** and **2k″** are almost degenerated. Similar to 2-furoyl thiourea, *m*-trifluoromethyl thiourea exhibits preponderance of the thione form (**3a**) over the thiol forms.[135] Moreover, the hyperconjugation effect is also observed in the case between **3a′** and **3a″**. However, in this case, stabilization of **3a′** → **3b′** by isomerization is attributed to a long-range SH···π interaction.[136−138] A simple compound from the family of 1-acyl thioureas has been reported recently;[139] intramolecular hydrogen bond also occurs in this species, between the carbonyl (C=O) and thioamide ($-NH_2$) groups, explaining tautomeric equilibria.[139]

https://doi.org/10.1021/acs.inorgchem.1c01068
Inorg. Chem. 2021, 60, 11984−12000

Scheme 3. Tautomeric Equilibria of the 2-Furoyl and *m*-Trifluoromethylphenyl Thiourea Derivatives[a]

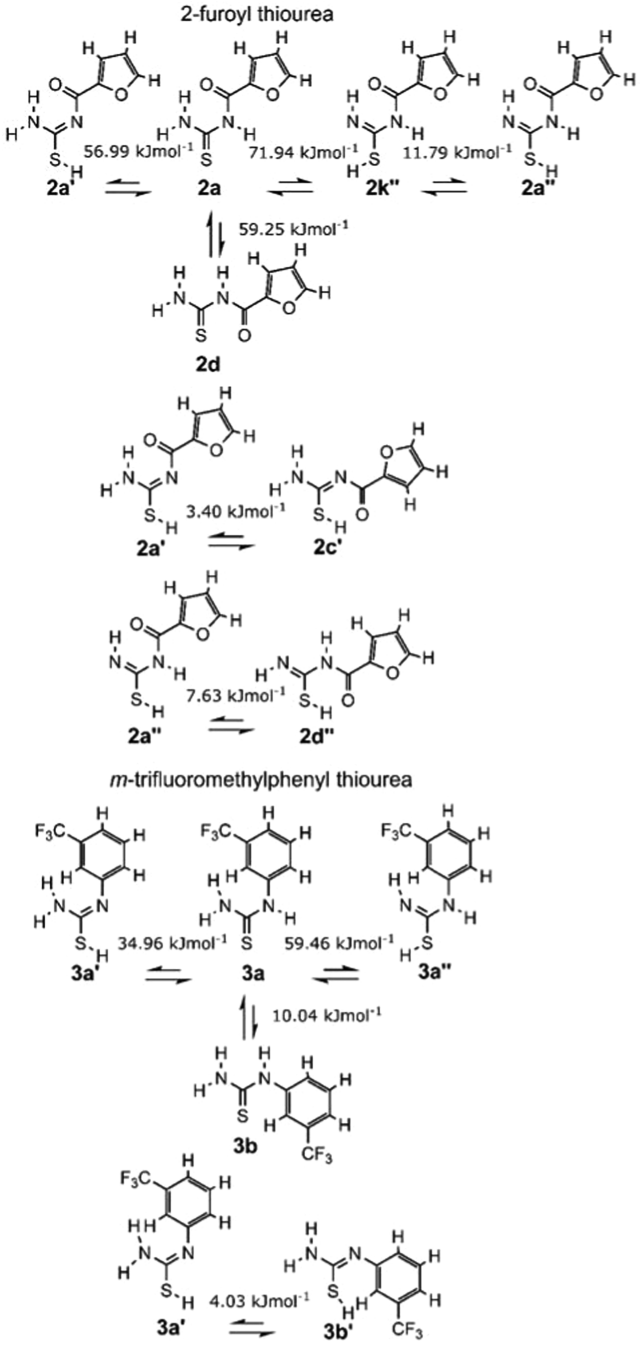

[a]Small arrows identify the less favorable reaction in the equilibrium. Relative Gibbs free energy between both forms in each equilibrium is given in kJ·mol^{-1}; notice that it does not correspond to the taumerization barriers.

Although intramolecular interactions play a key role in stabilizing structures **2a**, **2c**′, **3a**, and **3b**′, the stronger cation−molecule interactions mainly occur with other thione−thiol derivatives. Scheme 4 displays the representation of the most relevant cation−molecule complexes (further details of the structure of all studied complexes are given in the Supporting Information). Considering the thione/thiol derivatives bonded to the cations, we can infer that complex formation depends on the nucleophilic centers available in the molecule. A

Scheme 4. Most Stable Cation−Molecule Interactions for the 2-Furoyl and *m*-Trifluoromethyl Thiourea Derivatives[a]

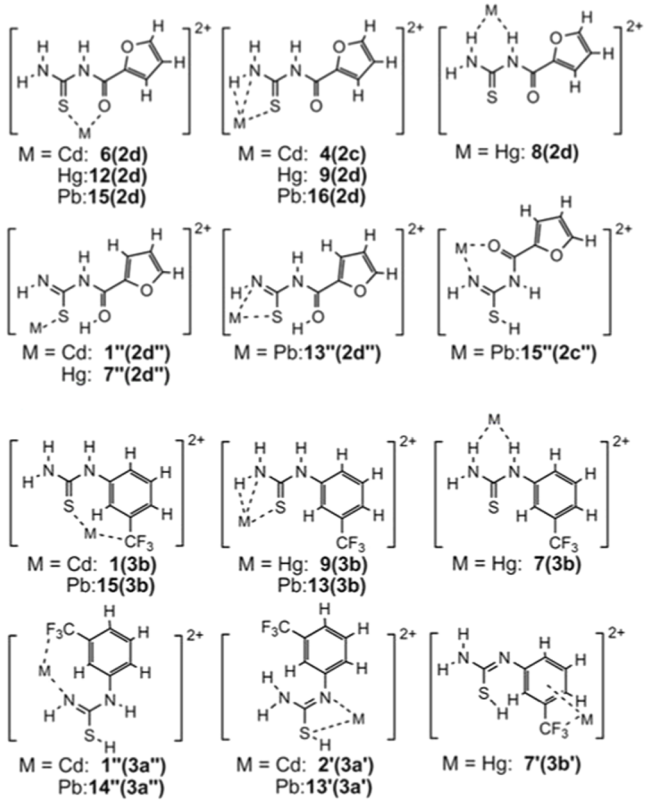

[a]Thiol forms are described by the superscript notation. Numbers have been added to identify the different sets of positions of the cations with respect to the molecules Cd: 1−6, Hg: 7−13, and Pb: 14−18.

comparison between the molecular structures in 3 and 4 allowed us to reinforce this assumption. Except for **3b**′, the remaining cation−molecule complexes are stabilized through interactions between the metal cation and the free electron-donor atoms; intramolecular interactions observed in 3 prevent these electron-donor atoms from being available as nucleophilic centers.

Table 3 gives complexation energies and the charge localized on the metal for the cation−molecule complexes with the lowest Gibbs free energy either with thione or with thiol forms. According to the energetic values observed, the number of available nucleophilic centers is not the only aspect controlling the cation−molecule binding, but the chemical nature of these

Table 3. Gibbs Free Energy of Formation (ΔG) and Cation Charge (q) for the Most Stable Cation−Molecule Complexes of the 2-Furoyl and *m*-Trifluoromethylphenyl Tautomers

	thione			thiol	
	ΔG (kJ mol^{-1})	q (e^-)		ΔG (kJ mol^{-1})	q (e^-)
Cd 6(2d)	−848.7	1.22	**Cd 1″(2d″)**	−743.1	1.03
Hg 9(2d)	−1012.3	0.31	**Hg 7″(2d″)**	−863.6	0.76
Pb 15(2d)	−652.2	1.39	**Pb 15″(2c″)**	−611.5	1.50
Cd 1(3b)	−783.0	1.12	**Cd 1″(3a″)**	−750.7	1.30
Hg 7(3b)	−967.6	0.90	**Hg 7′(3b′)**	−905.9	0.56
Pb 15(3b)	−532.8	1.29	**Pb 14″(3a″)**	−522.4	1.41

https://doi.org/10.1021/acs.inorgchem.1c01068
Inorg. Chem. 2021, 60, 11984−12000

centers is also relevant in the interaction strength between the cation and the molecule. Complexes formed with 2-furoyl thiourea (**2**) exhibit lower Gibbs free energies than those formed with *m*-trifluoromethyl thiourea (**3**). This is due to the presence of the oxygen atoms in **2** that are more polarizable and, therefore, share more easily the electron density than the fluorine atoms in **3**. In other words, the oxygen atoms act as nucleophilic centers with higher metal−cation affinity, in particular, the carbonyl one. Some exceptions are found for thiol forms of complexes with **3**, which appear more stable than those with **2**. This is the case for **1″(2d″)** and **1″(3a″)** and **7″(2d″)** and **7′(3b′)**. These exceptions reflect a different type of cation−molecule binding. While complexes **1″(3a″)** and **7′(3b′)** show bidentate interactions, **1″(2d″)** and **7″(2d″)** exhibit monodentate ones. One can intuitively think that the more the number of nucleophilic centers interacting with the cation, the stronger the interaction. Other interesting cases are **9(2d)** and **7(3b)**, where the cation−molecule interactions occur also through the H atoms.[140]

A close inspection of the cation charge (q) in Table 3 indicates an intense charge transfer process from the molecule to Hg(II). The strongest ones occur in **9(2d)** and **7′(3b′)** where Hg(II), which is connected to multiple nucleophilic centers, becomes almost neutral. The strength of the charge transfer is such that it can produce a reallocation of the electron density in the complex, allowing for the binding of Hg(II) even through two H atoms, as in **7(3b)** (see Figure 5). Charge transfer is also present in the complexes of Cd(II) and Pb(II) but to a lesser extent, and it does not show the same trend as in the case of Hg(II). In fact, **1″(2d″)** is the complex with the strongest charge transfer among those with Cd(II) and Pb(II), but, interestingly, the cation binds monodentally to the molecule. In general, Cd(II) can accept charge more easily than Pb(II) as seen by the (q) values in Table 3. This points out to different processes taking place in the interaction of the molecule within the three cations. While strong charge transfer with a predominance of electrostatic interactions strengthens the metal−molecule binding for Hg(II), in the case of Pb(II), the different chemical nature of the cation leads to a linkage with the nucleophilic centers that seems to present a higher covalent contribution, and it is likely that Cd(II) exhibits an intermediate behavior. We now analyze the structural properties and the bonding characteristics in the most relevant complexes to unveil the interaction nature.

Structural changes predicted upon complexation with thioureas were first reported in the neutral monocoordinated mode of acyl thiourea toward Au(I).[141] Structural modifications of the molecules induced by the cations also reflect differences between Cd(II), Hg(II), and Pb(II). Fully optimized models of the most stable cation−molecule complexes are displayed in Figure 5; for further representations, we refer the reader to the Supporting Information. The bidentate interaction of Cd(II) and Pb(II) in **6(2d)** and **15(2d)** modifies the molecule resulting in a planar structure with ∠CNCO = −0.02 and 0.07°, respectively. Similarly, in **9(2d)**, ∠CNCO = 0.07°. However, Hg(II) bidentally interacts with S and H inducing cyclization of the molecule. A simple visual inspection of **9(2d)** and **16(2d)** allows for understanding the difference between Cd(II), Pb(II), and Hg(II). It is important to point out that the **9(2d)** structure is analogous for Cd(II), although it is not more stable for this cation (see **4(2c)** in Scheme 4). In **9(2d)**, ∠HNH = 119° and for Cd(II), ∠HNH = 116°; therefore, NH_2 retains its sp^2 character.

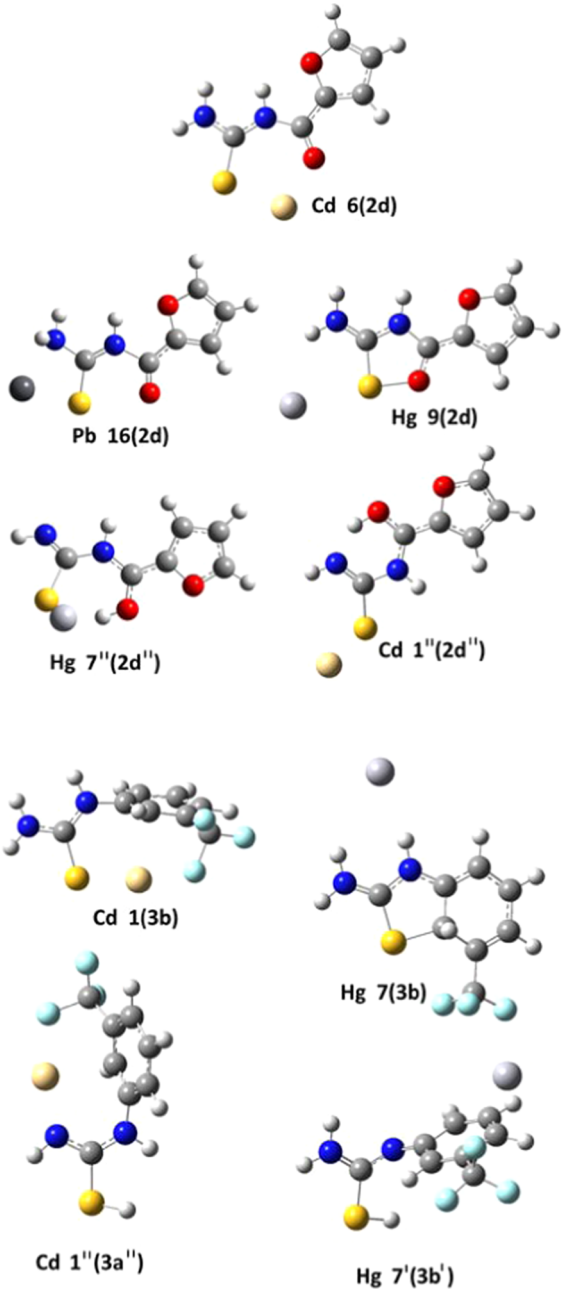

Figure 5. Full geometry-optimized structures of the cation−molecule complexes are denoted in Table 3. Model **15(2d)** has been omitted as it is analogous to **6(2d)** and, similarly, **15(3b)** and **14″(3a″)**, which are analogous to **1(3b)** and **1″(3a″)**, respectively. Model **16(2d)** has been included for comparison with **9(2d)**.

However, this hybridization is broken in **16(2d)** as shown by ∠HNH ∼108°, i.e., close to tetrahedral geometry. For the thiol forms **1″(2d″)** and **7″(2d″)**, the common features are the molecular flatness and formation of a hydroxyl (OH) group caused by the migration of a proton from the SH (see Scheme 4). Despite the cations being S-monodentally bonded to the molecule in both models, we do not observe any other structural similarities. The bidentate interaction of Hg(II) in **7(3b)** resembles that in **9(2d)**, causing the same cyclization of the molecule. Cd(II) and Pb(II) bidentally bind to the nucleophilic centers available (S and F) in **1(3b)** and **15(3b)**, respectively. In **1″(3a″)**, the cation strongly interacts with N and F atoms, which is reflected in ∠CdNH = 120° and

https://doi.org/10.1021/acs.inorgchem.1c01068
Inorg. Chem. 2021, 60, 11984−12000

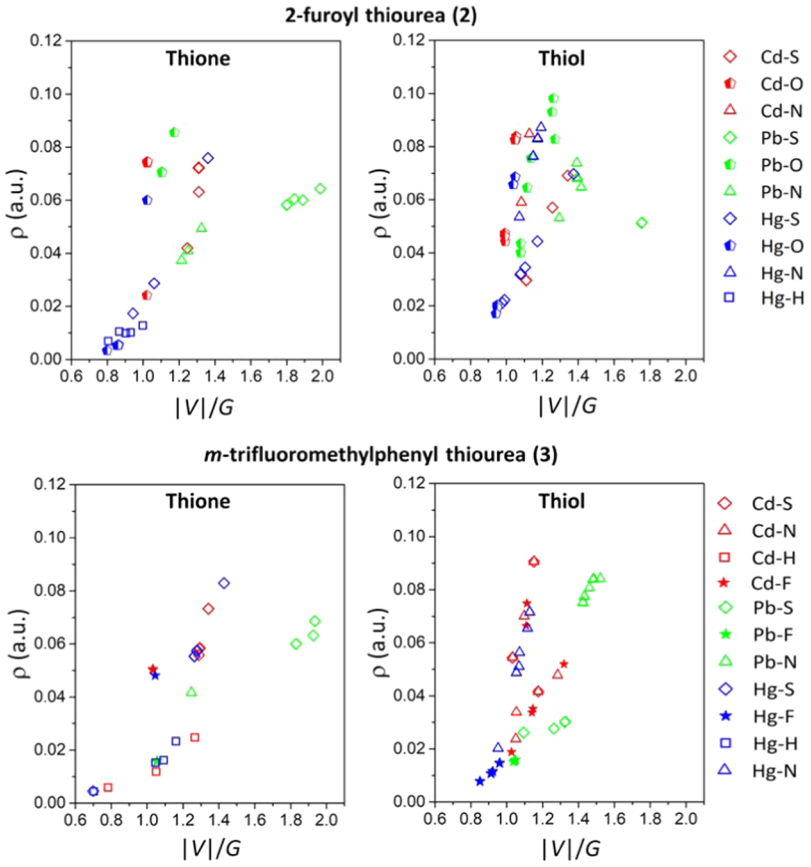

Figure 6. Plots of ρ vs $|V|/G$ for the more common BCPs of thione and thiol forms of each thiourea derivative. Ten most stable structures either in their thione or thiol forms have been used for graphical representation. Cation−molecule BCPs are distinguished using color, and symbols denote the specific atoms connected.

elongation of the C−F bond in ∼0.18 Å. Finally, modification of the π electron density of the phenyl ring in **7′**(**3b′**) upon complexation with the cation is clearly shown in the loss of the SH···π interaction (see Supporting Information). All of these observations indicate that Pb(II) interacts with the molecules, mainly leading to big changes in the chemical nature of the nucleophilic centers. On the other hand, the structural modifications induced by Hg(II) are mainly caused by the huge charge transfer. For Cd(II), both effects are simultaneously observed.

So far, we have been able to identify two processes involved in the cation−molecule interaction: charge transfer and the chemical nature of the nucleophilic centers. However, the trends observed have been only analyzed for those complexes in Table 3. To gain a deeper understanding of the cation−molecule interactions, a wider set of structures is needed. For this purpose, we applied the quantum theory of atoms in molecules (QTAIM) over the 10 most stable thione and thiol structures for each cation. For all of them, electron density properties at the BCPs have been computed. Similar to the case of nonsubstituted thiourea, we have focused on two descriptors ρ and $|V|/G$, which provide the bonding strength and the covalent/ionic character in the cation−molecule interaction, respectively.[115,116] In Figure 6, we present ρ as a function of $|V|/G$ for the cation−molecule complexes with the 2-furoyl (**2**) and *m*-trifluoromethyl (**3**) thioureas. Cations have been denoted with different colors. Symbols are used to label the more relevant bonds.

Most of the BCPs in bonds formed between thione structures of **2** and Hg(II) lie below or close to $|V|/G$ = 1.0; for Cd(II), it is close to 1.0−1.3, and in Pb(II), it exhibits greater dispersion ranging from 1.1 to 2.0. These findings show that the chemical nature of Hg(II) bonding is mainly ionic. Otherwise, Pb(II) and Cd(II) can show either a more ionic or more covalent character, achieving in some cases a noticeable covalent bonding ($|V|/G \geq 2$). This is in agreement with our aforementioned discussion, which described charge transfer as the main factor in the Hg(II)−molecule interaction. In terms of the bonding strength (ρ at the BCPs), the strongest interaction in Hg(II) complexes is found for the Hg−S bond, followed by the Hg−O one. Interestingly, Hg(II) is the only cation exhibiting a weak Hg−H ionic interaction, which is likely evidence of the charge transfer taking place through the H atoms. The ordering in the bonding is the opposite in Cd(II) and Pb(II) as compared to Hg(II), with first the cation−O and then the cation−S bonds. As expected, the Pb−S bond had the highest covalent character (see the preceding section). Noteworthily, only Pb(II), of the three cations, is able to interact with the thione forms of **2** through Pb−N bonds.

The interactions between the cations and the thiol forms of **2** are concentrated in the range of $|V|/G$ = 0.9−1.4, except for Pb−S interaction caused by the proton migration of the SH group (see **13″**(**2d″**) and **13″**(**2c″**) in Figure S6 and Table S4). The studied bonds in the considered structures have a mixed character, closer to ionic than to covalent interaction, except for Pb(II) complexes that are slightly more covalent. In terms of strength, the cation−S bond is the weakest

https://doi.org/10.1021/acs.inorgchem.1c01068
Inorg. Chem. 2021, 60, 11984−12000

interaction, likely due to the fact that more electron density is available for the bonding in the other nucleophilic centers, since, in the thiol forms, the S atom is compromised in the SH group or in S···HO hydrogen bonding. Indeed, contrary to what was observed for the thione form, in thiol complexes, Cd(II) and Hg(II) bind strongly to the O and N atoms, even more than Pb−N. However, similar to the thione form, Pb−O remains the strongest in the thiol form.

The lower number of points in the plot of ρ vs $|V|/G$ for thione structures of *m*-trifluoromethyl thiourea (**3**) reflects the lack of nucleophilic centers interacting with the cations. For the three metal atoms, the interaction cation−F, mostly ionic, is observed only in a few cases, indicating the difficulty to donate electrons from the F atoms.[142] The cation−S bond is the main interaction with a similar ionic/covalent character as observed in the thione forms of **2**. However, in thione **3**, Cd−H and Hg−H are present and show a lower extent of ionic character than for thione **2**, with values in some cases above $|V|/G = 1.0$. As was previously pointed out, here also, Pb(II) is the only cation with a Pb−N interaction. Values of ρ indicate stronger bonding of the cation−S interaction, which is explained by the easier polarizable electron density of the S atom. In comparison, Cd−H and Hg−H are mainly weak interactions that likely exist due to the cation−molecule charge transfer process.

Clearly, modification of **3** in the thiol structures produces a change in the chemical properties of the nucleophilic centers, as can be inferred from the increase of points in the ρ−$|V|/G$ plot. This stands out in the cation−F and cation−N interactions that were hardly present in the thione forms. On the other hand, Cd−H and Hg−H interactions completely disappear, suggesting that the main reason for Hg bonding in thione, charge transfer, strongly depends on the chemical environment of the linkage points. The former assumption is reinforced by the appearance of a weak Hg−F ionic interaction in the thiol forms, which points to charge transfer taking place through the F atoms. Another consequence of the electron-density loss in the S atom, caused by the SH bond in thiol forms, is the increase in the ionic character of the Pb−S interaction. The strongest bonds, the highest ρ values, occur for the cation−N interactions in the order Cd > Hg > Pb. This increasing trend can be explained using a simple hard/soft−acid/base principle.[143,144] Cd(II) is a softer acid than Hg(II) and subsequently Pb(II). Therefore, N atom being a softer base than F and O atoms, the Cd−N interaction is stronger.

Representation of the BCPs in Figure 7 demonstrates that cation−molecule formation induces the appearance of nonexistent intramolecular interactions in the bare molecules (without cations). Structures **15**(**2d**) and **15**″(**2c**″) exhibit NH···O hydrogen bonding with the furan ring. Such interactions were not present in the free molecules **2d** and **2c**″. Furthermore, in 2-furoyl thiourea, the NH···O hydrogen bonding using the furan ring is uncommon,[145,146] and in the metal complexes, it appears frequently. Interestingly, for **1**(**3b**) and **14**″(**3a**″), BCP representation allowed us to distinguish a tridentate interaction where the cations bind to the C atom in the *ortho*-position in the phenyl ring. Similarly, the bidentate interaction in **7**′(**3b**′) also shows the binding of the cation with the phenyl ring but in this case to the C atom in the *para*-position. Clearly, these observations reflect the ability of the cation to provoke charge reordering in the molecules despite the deactivating effect of the CF_3 group in the *meta*-position.[147,148]

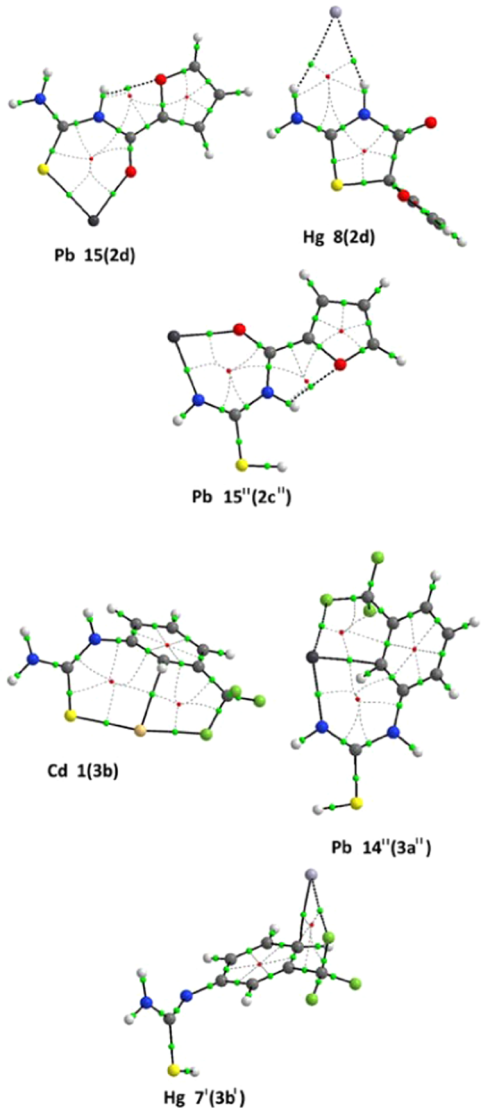

Figure 7. Representation of the BCPs (green) in the structures where peculiar binding sites are noted. Ring critical points (red) and bond paths (dashed line) are included. The atom radius and bonds have been modified for better visualization of the critical points.

Chemical Synergy of *N,N*′-Disubstitution. The joining of both substituents to different N atoms results in a new compound, *N*-(2-furoyl)-*N*′-(*m*-trifluoromethyl)-phenylthiourea (**4**), with new chemical features. First, the intramolecular hydrogen migration provoked by tautomerization can occur through any of the −NH groups connected to each fragment.[149] We have denoted the tautomers according to the hydrogen migration direction. If the hydrogen is released by the −NH group joined to the *m*-trifluoromethylphenyl substituent, a double superscript notation is used, and if migration occurs from the −NH group joined to the 2-furoyl substituent, we have employed a single superscript notation. Thiones and thiol forms of **4** are illustrated in Figure 8. According to the results of the previous section, a wide set of structures is needed to understand the cation−molecule interaction. Therefore, another group of structures has been included besides the more stable ones for each form, namely, **4f**, **4a**′, and **4a**″.

Isomerization of the most stable isomer, **4f**, into the subsequent thione structures reflects the breakdown of the

https://doi.org/10.1021/acs.inorgchem.1c01068
Inorg. Chem. 2021, 60, 11984−12000

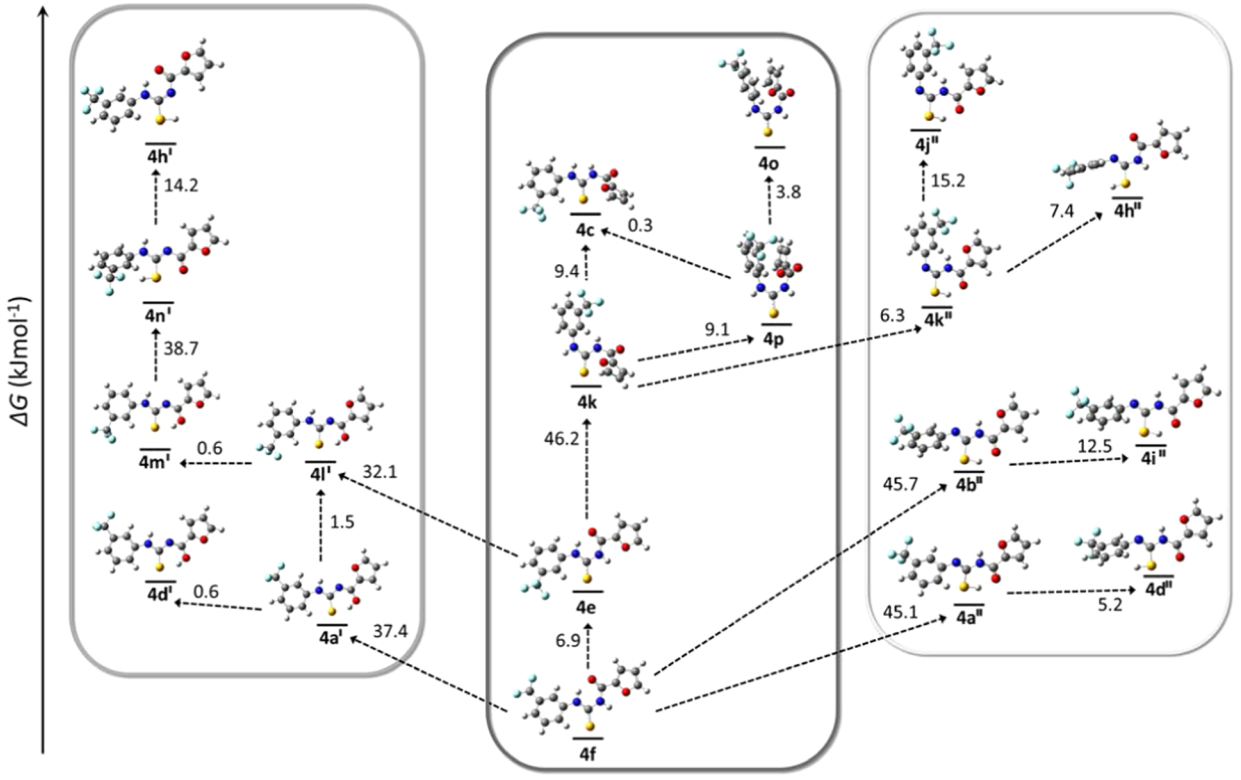

Figure 8. Energetic paths of the main tautomeric forms of *N*-(2-furoyl)-*N*′-(*m*-trifluoromethyl)phenylthiourea (**4**). Thiol forms are distinguished from the thione form by superscript notations. Relative Gibbs free energy between both forms in each equilibrium is given in kJ·mol^{-1}; notice that it does not correspond to the tautomerization barriers.

intramolecular interactions, especially hydrogen bonding. This is remarkable in the **4e** → **4k** isomerization with the disappearance of both NH···O bonds. Consequently, the loss of intramolecular interactions destabilizes the structure, and an increase of almost 40 kJ·mol^{-1} in the Gibbs free energy is obtained. However, the resulting structures of such isomerization allowed us to obtain precursors to achieve different stable tautomeric forms. Starting from **4f**, **4e**, and **4k**, a diversity of thiol forms of type **4**′ and **4**″ were found. Despite having two types of thiol forms, some structural similarities are preserved. Structures **4a**′ and **4a**″ differ in the intramolecular hydrogen migration, which in the case of **4a**′ results in the formation of a hydroxyl group (−OH), causing higher stability against **4a**″. A double hydrogen bond with the S atom, CH···S and OH···S, further stabilizes **4a**′ with respect to **4a**″.[150,151] In fact, the double effect of the hydrogen bonds allows for isomerization of **4a**′ into **4d**′ and **4m**′ with very low energetic thresholds. In contrast, the isomerization of **4a**″ → **4d**″ requires more energy since it implies cleavage of the SH···O bond.[13,151] Nevertheless, it is possible to find energetic paths of analogous thiol forms where intramolecular interactions are discarded due to −OH formation. Furthermore, the formation of the −OH bond is also remarkable since nucleophilic centers N and O atoms remain free and can be important anchoring points for the binding of the cation to the molecule. Further isomerization leads to the formation of thiol structures **4h**″ or **4h**′, which, although very unstable, have available lone pairs in the N and O atoms to bind with the cations. All of these structures have been considered in metal-complexation studies. In the case of complexation with disubstituted species, the steric demand of the ligand toward metal coordination must be taken into account.[152]

A full study of the cation−molecule interaction strength cannot be accomplished by analyzing only the structures of the most stable complexes. Therefore, aiming to obtain a deeper understanding, we have considered ∼13 structures in each case, i.e., for each of the three metal cations interacting with thiourea either in its thione (**4**) or thiol (**4**′ and **4**″) forms using the conformers in Figure 8. In total, we have analyzed 37, 43, and 38 structures for Pb(II), Cd(II), and Hg(II), respectively. To do this, we grouped those lying within an energy range of 15 kJ·mol^{-1} to construct the histogram plots shown in Figure 9. The charge hosted by the cation (q) in each complex is also shown in the figure.

For the three cations, the complexes formed with the thione form **4** are more stable than those with any of the thiol structures **4**′ and **4**″. A large number of structures lying at lower energies with **4** can be noticed. This is due to the fact that typically S and O atoms in the thiones are available to bind with the cations, resulting in strong interactions, while in thiol forms, these atoms appear as −SH or −OH groups. Furthermore, differences in the relative stability of structures formed between the two thiol forms can also be distinguished. Complexes with **4**′ show higher stability with respect to those with **4**″ for Cd(II) and Hg(II). However, for Pb(II), complexes with **4**′ are mainly in the range from −500 to −620 kJ·mol^{-1}, while some with **4**″ appear below −620 kJ·mol^{-1}. This behavior reflects the preference of Pb(II) to bidentally bind to close free nucleophilic centers such as N and O atoms[153] (see Figure 7 and the Supporting Information). The O atom in the carbonyl group of the **4**′ structures is compromised in −OH formation or in an NH···O hydrogen bond (see, e.g., **4d**′ and **4h**′ in Figure 7) and, consequently, this site, which is the one to which Pb binds most strongly, is

https://doi.org/10.1021/acs.inorgchem.1c01068
Inorg. Chem. 2021, 60, 11984−12000

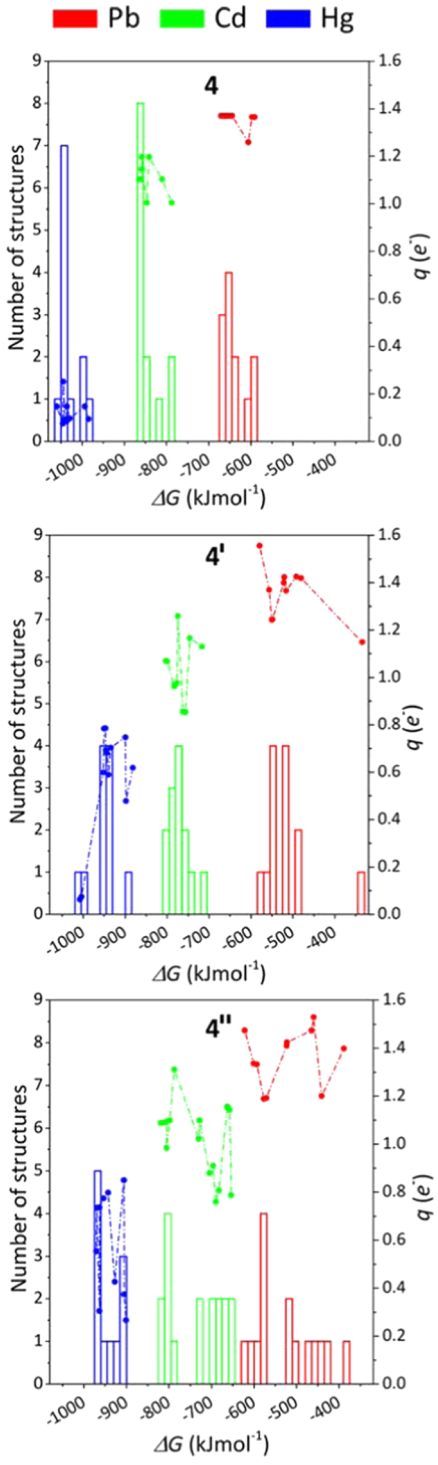

Figure 9. Number of structures vs ΔG, histograms and cation charge (q) vs ΔG, dashed-dotted lines. Colors have been used to identify the complexes of each cation, and the corresponding tautomeric forms are given in each panel: upper **4**, medium **4′**, and lower **4″**.

occupied, thus weakening the cation−molecule interaction[154,155] (see also the previous section on the effects of N-monosubstitution).

Although no clear trends are observed in the cationic charge, q, vs ΔG graphs, it is possible to highlight some general aspects that differentiate each cation. Clearly, charge transfer occurs to a greater extent in complexes formed with Hg(II). Values of q in Figure 9 can almost achieve the neutral oxidation state, especially for those formed with the thione form **4**, where $q <$ 0.2 in most cases. Complexes of Hg(II) with the thiol forms (either **4′** or **4′**) also reach low q values ($q < 0.8$). On the other hand, the charge donation from the molecule to the cation takes place at a different level for Cd(II) and Pb(II); in Cd, the charge $q \sim 1.0$, and in Pb, it is slightly higher, $q \sim 1.4$. These results imply that charge transfer is dominant in Hg(II) and has a minor effect on Cd(II) and even less on Pb(II), which is in agreement with our observations in previous sections.

Using QTAIM, we have performed an in-depth analysis of the bonding properties for the most stable complexes (see Figure 10 and Table 4). Depending on the metal, the interaction with the molecule is chemically specific. Cd(II) binds to C, S, and F atoms to form tridentate complexes, regardless of the tautomeric form of the molecule, being the only cation achieving such a level of complexation. In the case of **2″**(**4b″**), the Cd−molecule interaction changes the S−H−O bonding properties, while in the free molecule, hydrogen bonding takes place with the oxygen atom, S−H···O (see **4b″** in Figure 7) and in the complex, it takes place with the sulfur atom, S···H−O. As already shown in the previous section, Hg(II) has a clear preference to interact with H atoms. Interestingly, Hg(II) produces strong structural modifications that result in the cyclization of the molecule through the S and C-*ortho* atoms. Similar cyclization induced by cation has been previously reported for other molecules.[156−158] A comparison between **10′**(**4d′**) and **9**(**4o**) points out that such a cyclization process depends on the binding of cation to the H atom and, in fact, we have also obtained other cyclic structures with Hg(II) complexes (see Supporting Information). Nevertheless, cyclization probably requires a particular orientation of the *m*-trifluoromethylphenyl fragment with respect to the S atom because in **7″**(**4b″**), it is not seen. Finally, Pb(II) is the most chemospecific of the three cations, with a preference for S, N, and O as linkage sites; in some cases, a disruption in the structure of the free molecule is imposed with complexation (see, e.g., **15**(**4k**) in Figure 10 and **4k** in Figure 7).

From Table 4, we can obtain further insight into the cation−molecule interaction of the structures shown in Figure 10. The three bonds between the metal and the molecule present very similar characteristics when Cd(II) forms a complex with the thione or thiol forms. Indeed, the values of q, ρ, and $|V|/G$ are almost identical in each bond for the three structures. We can thus conclude that the cation bonding strength is analogous for the three Cd(II) complexes. Therefore, the difference between them in terms of relative energy relies on the intramolecular forces, **3**(**4p**) being most stable with two H bonds involving both oxygen atoms of the furoyl group. In the case of Hg(II), we clearly observe that complexation is enhanced by charge transfer. High stabilization (see ΔG) is accompanied by very low q for **10′**(**4d′**) and **9**(**4o**). In these two structures, the cation is bonded to a H atom, with the value of $|V|/G$ close to 1, indicating ionic character in both Hg−H bonds. However, structure **7″**(**4b″**) shows some differences: Hg(II) is in this case bonded to S and C atoms and although the Hg−S and Hg−C bonds exhibit the same degree of ionicity ($|V|/G \sim 1$), the bonds have a higher electron density in BCP, ρ_{BCP}, and the charge is slightly higher in the metal ($q_{Hg} = 0.55$). Finally, for Pb(II) complexes, the ΔG values reflect that the cation preference for O atoms can also depend on the chemical nature of the binding sites. We observe a noticeable difference in the cation bonding strength to the O atoms in the carbonyl and the furan ring. In fact, the smallest ρ value is observed at

https://doi.org/10.1021/acs.inorgchem.1c01068
Inorg. Chem. 2021, 60, 11984−12000

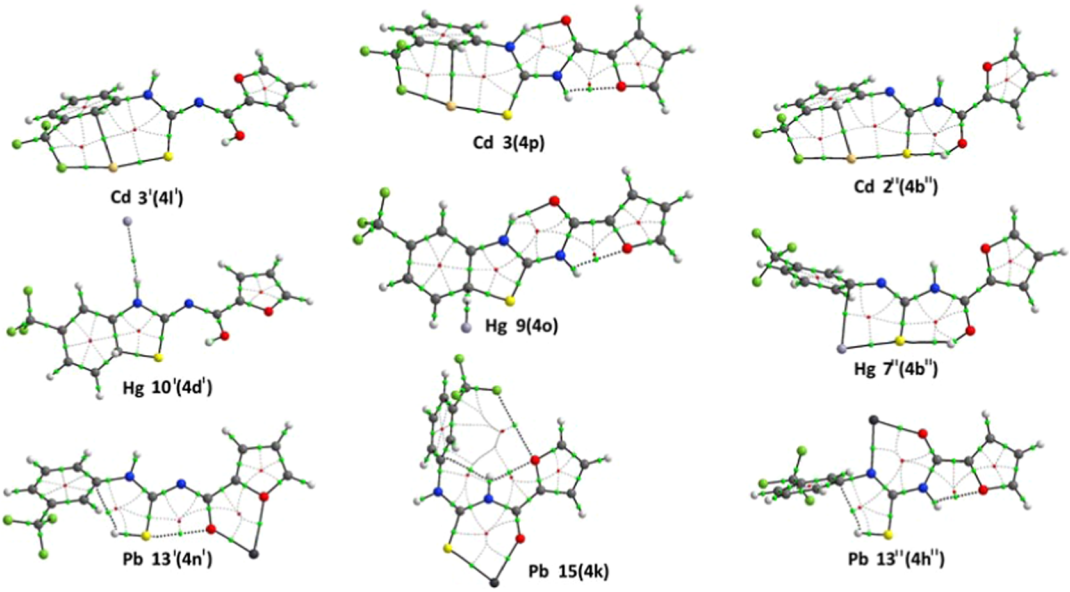

Figure 10. Structures of the most stable complexes of *N*-(2-furoyl)-*N*′-(*m*-trifluoromethyl)phenylthiourea (**4**) at its different tautomeric forms. The bond critical points (BCPs) are represented by green dots and the ring critical points by red dots. In addition, the dashed lines describe the bond paths.

Table 4. Gibbs Free Energies (ΔG) in kJ mol^{-1}, Electron Density Properties at the BCPs (ρ, $|V|/G$) in Atomic Units, and Cation Charge (q) for the Structures in Figure 10

	ΔG	q	BCPs	ρ	$\lvert V\rvert/G$
3(4p)	−865.6	1.10	Cd−S	0.074	1.34
			Cd−F	0.048	1.03
			Cd−C	0.040	1.16
3′(4l′)	−803.2	1.07	Cd−S	0.075	1.34
			Cd−F	0.046	1.04
			Cd−C	0.039	1.16
2″(4b″)	−819.2	1.09	Cd−S	0.071	1.32
			Cd−F	0.041	1.05
			Cd−C	0.051	1.24
9(4o)	−1059.8	0.15	Hg−H	0.021	1.12
10′(4d′)	−1008.0	0.06	Hg−H	0.013	1.01
7″(4b″)	−970.7	0.55	Hg−S	0.044	1.18
			Hg−C	0.025	1.01
15(4k)	−671.0	1.37	Pb−S	0.060	1.82
			Pb−O[a]	0.072	1.11
13′(4n′)	−579.7	1.55	Pb−O[a]	0.099	1.26
			Pb−O[b]	0.040	1.08
13″(4h″)	−622.3	1.47	Pb−N	0.075	1.43
			Pb−O[a]	0.075	1.14

[a]Oxygen atom of carbonyl. [b]Oxygen atom of the furan ring.

the BCP of the Pb−O bond with furan in **13′(4n′)**. This is understood by the higher electron density present in the O atom of carbonyl than in that of furan.[159] Accordingly, the higher ionic character of the Pb−O bond in furan is also indicative of this difference in electron density.

The small ρ values in the BCPs obtained in the bonds involving Hg reflect the lowest bond strengths, an apparently contradictory fact if we consider that the highest complexation Gibbs free energies are obtained for this metal. Even in the case of **10′(4d′)**, where the only anchoring point is a weak Hg···H bond, stabilization of this complex with more than 1000 kJ·mol^{-1} is observed. Precisely, Hg complexes are those with the highest electron density transferred from the molecule to the cation (lowest q_{metal}), highlighting the importance of charge transfer.

CONCLUSIONS

In conclusion, we have theoretically studied the complexation of three metal cations, namely, Cd(II), Hg(II), and Pb(II), with four thiourea molecules: (**1**) bare thiourea, (**2**) 2-furoyl thiourea, (**3**) *m*-triflouromethylphenyl thiourea, and (**4**)*N*-(2-furoyl)-*N*′-(trifluoromethyl)phenylthiourea; both the thione and the thiol forms of these compounds have been considered. Several isomers were computed for each compound, giving a total of 479 structures (all shown in the Supporting Information). The analysis of the interaction energies and bonding properties was carried out for the most stable structure in each case. A summary of the complexation Gibbs free energy is given in Figure 11. Hg(II) is the ion with higher binding energy, followed by Cd(II) and Pb(II). The thione conformers are most stable in each case, except for the complex of Pb(II) with the bare thiourea (**1**), where the thiol form is slightly more stable. *N*-monosubsituted thioureas lead to higher stabilization than the bare thiourea, (**2**) being more stable than (**3**) for the thiones and the thiols with Pb and (**3**) more stable than (**2**) for the thiols with Cd and Hg. In all cases, *N*,*N*′-disubstitution is accompanied by a remarkable stabilization of the complex, showing the synergy effect of both substituent groups. This effect is especially marked in the case of Hg, for which an increase in stabilization of up to 260 kJ·mol^{-1} can be seen with respect to the nonsubstituted thiourea. The higher affinity of the proposed thiourea derivatives to form a complex with Hg(II) is mainly due to the large amount of charge transferred in such complexes, which, in some cases, leads to total neutralization of the cation. In other words, the higher oxidizing capacity of Hg(II) leads to a molecule^{2+}···Hg compound, where the charge is stabilized in the molecule, mainly along the thiourea N_2CS core. This is in contrast with the weaker bonds that Hg(II) establishes with the molecule, which are mainly Hg−H bonds, while Pb(II) and Cd(II) form

https://doi.org/10.1021/acs.inorgchem.1c01068
Inorg. Chem. 2021, 60, 11984−12000

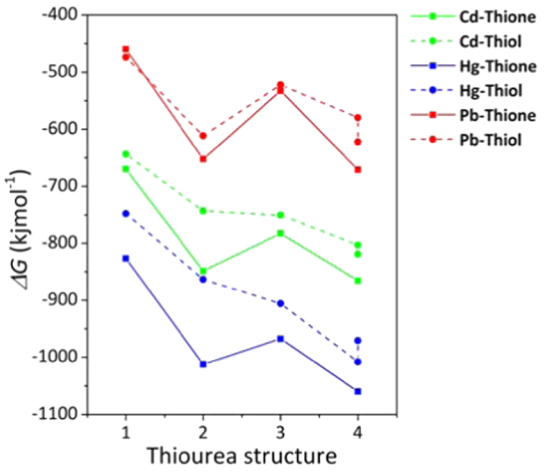

Figure 11. Gibbs free energy of complexation, ΔG (in kJ·mol^{-1}), for the most stable conformer formed in the interaction of each considered cation Cd, Hg, and Pb with the thione or thiol forms of the four studied thiourea structures: (**1**) bare thiourea, (**2**) 2-furoyl thiourea, (**3**) *m*-triflouromethylphenyl thiourea, and (**4**) *N*-(2-furoyl)-*N*′-(*m*-trifluoromethyl)phenylthiourea.

stronger bonds with nucleophilic centers such as S, O, or N atoms. The proposed *N*,*N*′-disubstituted thiourea is thus a potential candidate to be implemented in heavy metal ion sensors and for the removal of these cations. Of particular interest is the higher affinity for binding Hg(II) through H atoms, since the S atom of thiourea is free to be anchored to a support, for instance, a metal surface. This can be part of an effective nanosensor simply by connecting the metal with the processing circuit for electronic control. We hope that the results reported in this work stimulate further studies with the aim of including solvent effects, which are expected to be highly important in metal−cation complexation by disubstituted thioureas.

■ ASSOCIATED CONTENT

Supporting Information

The Supporting Information is available free of charge at https://pubs.acs.org/doi/10.1021/acs.inorgchem.1c01068.

Representation of the 479 cation−molecule structures considered in the study; detailed information of all conformers and tautomers obtained; examples showing the local charge of the Hg−H interaction; solvent effects; and comparison of exchange−correlation functionals B3LYP *vs* ωB97XD (PDF)

■ AUTHOR INFORMATION

Corresponding Author

Sergio Díaz-Tendero − *Departmento de Química, Módulo 13 and Condensed Matter Physics Center (IFIMAC), Universidad Autónoma de Madrid, 28049 Madrid, Spain; Institute for Advanced Research in Chemical Science (IAdChem), Universidad Autónoma de Madrid, 28049 Madrid, Spain;* orcid.org/0000-0001-6253-6343; Email: sergio.diaztendero@uam.es.

Authors

Ransel Barzaga − *Instituto de Ciencia y Tecnología de Materiales, Universidad de La Habana, 10400 La Habana, Cuba; Departmento de Química, Módulo 13, Universidad Autónoma de Madrid, 28049 Madrid, Spain*

Lucia Lestón-Sánchez − *Departmento de Química, Módulo 13, Universidad Autónoma de Madrid, 28049 Madrid, Spain*

Fernando Aguilar-Galindo − *Departmento de Química, Módulo 13, Universidad Autónoma de Madrid, 28049 Madrid, Spain; Donostia International Physics Center (DIPC), Donostia-San Sebastián E-20018, Spain;* orcid.org/0000-0003-2751-5592

Osvaldo Estévez-Hernández − *Instituto de Ciencia y Tecnología de Materiales, Universidad de La Habana, 10400 La Habana, Cuba*

Complete contact information is available at: https://pubs.acs.org/10.1021/acs.inorgchem.1c01068

Notes

The authors declare no competing financial interest.

■ ACKNOWLEDGMENTS

We acknowledge the generous allocation of computer time at the Centro de Computación Científica at the Universidad Autonóma de Madrid (CCC-UAM). R.B. acknowledges Fundación Carolina, Spain, for a Ph.D. fellowship. This work was partially supported by the MICINN, Spanish Ministry of Science and Innovation, project PID2019-110091GB-I00 and the "María de Maeztu" Program for Centers of Excellence in R&D (CEX2018-000805-M).

■ REFERENCES

(1) Gidlow, D. Lead toxicity. *Occup. Med.* **2004**, *54*, 76−81.

(2) Engwa, G. A.; Ferdinand, P. U.; Nwalo, F. N.; Unachukwu, M. N. In *Poisoning in the Modern World*; Karcioglu, O.; Arslan, B., Eds.; IntechOpen: Rijeka, 2019; Chapter 5.

(3) Tchounwou, P.; Yedjou, C.; Patlolla, A.; Sutton, D. Heavy metal toxicity and the environment. *Exper. Suppl.* **2012**, *101*, 133−64.

(4) Atieh, M. A.; Ji, Y.; Kochkodan, V. Metals in the Environment: Toxic Metals Removal. *Bioinorg. Chem. Appl.* **2017**, *2017*, No. 4309198.

(5) Masindi, V.; Muedi, K. L. In *Heavy Metals*; Saleh, H. E.-D. M.; Aglan, R. F., Eds.; IntechOpen: Rijeka, 2018; Chapter 7.

(6) Yang, Y.; Ali, H.; Khan, E.; Ilahi, I. Environmental Chemistry and Ecotoxicology of Hazardous Heavy Metals: Environmental Persistence, Toxicity, and Bioaccumulation. *J. Chem.* **2019**, *2019*, No. 6730305.

(7) Briffa, J.; Sinagra, E.; Blundell, R. Heavy metal pollution in the environment and their toxicological effects on humans. *Heliyon* **2020**, *6*, No. e04691.

(8) Special Issue "Advanced Sensors for the Detection of Heavy Metals". *Sensors* **2019**, *19*.

(9) Verma, N.; Singh, M. Biosensors for heavy metals. *Biometals* **2005**, *18*, 121−129.

(10) Ozkan, S. A.; Turdean, G. L. Design and Development of Biosensors for the Detection of Heavy Metal Toxicity. *Int. J. Electrochem.* **2011**, *2011*, No. 343125.

(11) Saidur, M.; Aziz, A. A.; Basirun, W. Recent advances in DNA-based electrochemical biosensors for heavy metal ion detection: A review. *Biosens. Bioelectron.* **2017**, *90*, 125−139.

(12) Peng, B.; Fang, S.; Tang, L.; Ouyang, X.; Zeng, G. In *Nanohybrid and Nanoporous Materials for Aquatic Pollution Control*; Tang, L.; Deng, Y.; Wang, J.; Wang, J.; Zeng, G., Eds.; Elsevier, 2019; pp 233−264.

(13) Aarabi, M.; Gholami, S.; Grabowski, S. J. S-H···O and O-H···O Hydrogen Bonds-Comparison of Dimers of Thiocarboxylic and Carboxylic Acids. *ChemPhysChem* **2020**, *21*, 1653−1664.

(14) Lin, M.; Cho, M.; Choe, W.-S.; Son, Y.; Lee, Y. Electrochemical detection of copper ion using a modified copolythiophene electrode. *Electrochim. Acta* **2009**, *54*, 7012−7017.
(15) Pujol, L.; Evrard, D.; Groenen-Serrano, K.; Freyssinier, M.; Ruffien-Cizsak, A.; Gros, P. Electrochemical sensors and devices for heavy metals assay in water: the French groups' contribution. *Front. Chem.* **2014**, *2*, No. 19.
(16) Dai, X.; Wu, S.; Li, S. Progress on electrochemical sensors for the determination of heavy metal ions from contaminated water. *J. Chinese Adv. Mater. Soc.* **2018**, *6*, 91−111.
(17) García-Miranda Ferrari, A.; Carrington, P.; Rowley-Neale, S. J.; Banks, C. E. Recent advances in portable heavy metal electrochemical sensing platforms. *Environ. Sci.: Water Res. Technol.* **2020**, *6*, 2676−2690.
(18) Sall, M. L.; Diaw, A. K. D.; Gningue-Sall, D.; Efremova Aaron, S.; Aaron, J.-J. Toxic heavy metals: impact on the environment and human health, and treatment with conducting organic polymers, a review. *Environ. Sci. Pollut. Res.* **2020**, *27*, 29927−29942.
(19) Xuan, X.; Hossain, M. F.; Park, J. Y. A Fully Integrated and Miniaturized Heavy-metal-detection Sensor Based on Micro-patterned Reduced Graphene Oxide. *Sci. Rep.* **2016**, *6*, No. 33125.
(20) Afreen, S.; Talreja, N.; Chauhan, D.; Ashfaq, M. In *Multifunctional Hybrid Nanomaterials for Sustainable Agri-Food and Ecosystems*; Abd-Elsalam, K. A., Ed.; Elsevier, 2020; pp 335−353.
(21) Ahmad, F.; et al. In *Metal Oxide Powder Technologies*; Al-Douri, Y., Ed.; Elsevier, 2020; pp 299−332.
(22) Buledi, J. A.; Amin, S.; Haider, S. I.; Bhanger, M. I.; Solangi, A. R. A review on detection of heavy metals from aqueous media using nanomaterial-based sensors. *Environ. Sci. Pollut. Res.* **2020**, 1.
(23) Czolk, R.; Reichert, J.; Ache, H. An optical sensor for the detection of heavy metal ions. *Sens. Actuators, B* **1992**, *7*, 540−543.
(24) van der Veen, N. J.; Egberink, R. J. M.; Engbersen, J. F. J.; Reinhoudt, D. N. Selective Optode Membranes for Heavy Metal Ion Detection. *Sensor Technology in the Netherlands: State of the Art*; Springer: Dordrecht, 1998; pp 107−110.
(25) Ranjbar, L.; Yamini, Y.; Saleh, A.; Seidi, S.; Faraji, M. Ionic liquid based dispersive liquid-liquid microextraction combined with ICP-OES for the determination of trace quantities of cobalt, copper, manganese, nickel and zinc in environmental water samples. *Microchim. Acta* **2012**, *177*, 119−127.
(26) Jerónimo, P. C.; Araújo, A. N.; Montenegro, M. B. Development of a sol−gel optical sensor for analysis of zinc in pharmaceuticals. *Sens. Actuators, B* **2004**, *103*, 169−177. The 17th Euopean Conference on Solid-State Transducers, University of Minho, Guimares, Portugal, September 21−24, 2003.
(27) Díez-Gil, C.; Caballero, A.; Ratera, I.; Tárraga, A.; Molina, P.; Veciana, J. Naked-eye and Selective Detection of Mercury (II) Ions in Mixed Aqueous Media Using a Cellulose-based Support. *Sensors* **2007**, *7*, 3481−3488.
(28) Vlascici, D.; Fagadar-Cosma, E.; Pica, E.; Cosma, O. V.; Bizerea; Mihailescu, G.; Olenic, L. Free Base Porphyrins as Ionophores for Heavy Metal Sensors. *Sensors* **2008**, *8*, 4995−5004.
(29) Ward, J.; Li, L.; Regan, F.; Deasy, M.; Kelleher, F. Bis(spirolactam) 1,3-double-armed calix[4]arene compounds and their application as extractants for the determination of heavy metal ions. *J. Inclusion Phenom. Macrocyclic Chem.* **2015**, *83*, 377−386.
(30) Khan, S. B.; Zamadar, M.; Orr, C.; Uherek, M. Water Soluble Cationic Porphyrin Sensor for Detection of Hg^{2+}, Pb^{2+}, Cd^{2+}, and Cu^{2+}. *J. Sens.* **2016**, *2016*, No. 1905454.
(31) Sun, L.; Sun, C.; Sun, X. Screening highly selective ionophores for heavy metal ion-selective electrodes and potentiometric sensors. *Electrochim. Acta* **2016**, *220*, 690−698.
(32) Otazo-Sánchez, E.; Pérez-Marín, L.; Estévez-Hernández, O.; Rojas-Lima, S.; Alonso-Chamarro, J. Aroylthioureas: new organic ionophores for heavy-metal ion selective electrodes. *J. Chem. Soc., Perkin Trans. 2* **2001**, 2211−2218.
(33) Otazo-Sánchez, E.; del Toro, P. O.; Estévez-Hernández, O.; Pérez-Marín, L.; Goicoechea, I.; Cerón Beltran, A.; Villagómez-Ibarra, J. Aroylthioureas: new organic ionophores for heavy metal ion selective electrodes. A nuclear magnetic resonance study. *Spectrochim. Acta, Part A* **2002**, *58*, 2281−2290.
(34) Yao, Z.; Li, J.; Xie, H.; Yu, C. Review on Remediation Technologies of Soil Contaminated by Heavy Metals. *Procedia Environ. Sci.* **2012**, *16*, 722−729. The Seventh International Conference on Waste Management and Technology (ICWMT 7)
(35) Selvi, A.; Rajasekar, A.; Theerthagiri, J.; Ananthaselvam, A.; Sathishkumar, K.; Madhavan, J.; Rahman, P. K. S. M. Integrated Remediation Processes Toward Heavy Metal Removal/Recovery From Various Environments-A Review. *Front. Environ. Sci.* **2019**, *7*, No. 66.
(36) Xu, J.; Liu, C.; Hsu, P.-C.; Zhao, J.; Wu, T.; Tang, J.; Liu, K.; Cui, Y. Remediation of heavy metal contaminated soil by asymmetrical alternating current electrochemistry. *Nat. Commun.* **2019**, *10*, No. 2440.
(37) Akhtar, F. Z.; Archana, K. M.; Krishnaswamy, V. G.; Rajagopal, R. Remediation of heavy metals (Cr, Zn) using physical, chemical and biological methods: a novel approach. *SN Appl. Sci.* **2020**, *2*, 267.
(38) Akün, M. E. In *Heavy Metal Toxicity in Public Health*; Nduka, J. K.; Rashed, M. N., Eds.; IntechOpen: Rijeka, 2020; Chapter 1.
(39) Schuster, M.; Koenig, K.-H.; Lotter, H.; Drauz, K. Substituted Thioureas for the Separation of Complexly Bound Heavy-Metal Ions.US Patent 4,980,0711990.
(40) Das, D. K. N-α-(5-bromopyridyl)-N′-benzoyl thiourea (BrPBT) as a new chelating agent for the spectrophotometric determination of rhodium(III). *Fresenius' Z. Anal. Chem.* **1984**, *318*, 612.
(41) Ammi Said, A.; Amara, M.; Kerdjoudj, H. The effect of thiourea as a complexing agent on the separation of metallic ions through cation exchange membranes by Donnan dialysis. *Ionics* **2013**, *19*, 177−183.
(42) Ravikumar, L.; Kalaivani, S.; Vidhyadevi, T.; Murugasen, A.; Kirupha, S.; Sivanesan, S. Synthesis, Characterization and Metal Ion Adsorption Studies on Novel Aromatic Poly(Azomethine Amide)s Containing Thiourea Groups. *Open. J. Polym. Chem.* **2014**, *4*, 1−11.
(43) Yao, X.; Wang, H.; Ma, Z.; Liu, M.; Zhao, X.; Jia, D. Adsorption of Hg(II) from aqueous solution using thiourea functionalized chelating fiber. *Chin. J. Chem. Eng.* **2016**, *24*, 1344−1352.
(44) Gomez, J. D. C.; Hagenbach, A.; Gerling-Driessen, U. I. M.; Koksch, B.; Beindorff, N.; Brenner, W.; Abram, U. Thiourea derivatives as chelating agents for bioconjugation of rhenium and technetium. *Dalton Trans.* **2017**, *46*, 14602−14611.
(45) An, F.-Q.; Wang, Y.; Xue, X.-Y.; Hu, T.-P.; Gao, J.-F.; Gao, B.-J. Design and application of thiourea modified D301 resin for the effective removal of toxic heavy metal ions. *Chem. Eng. Res. Des.* **2018**, *130*, 78−86.
(46) Cunha, B. N.; Colina-Vegas, L.; Plutín, A. M.; Silveira, R. G.; Honorato, J.; Oliveira, K. M.; Cominetti, M. R.; Ferreira, A. G.; Castellano, E. E.; Batista, A. A. Hydrolysis reaction promotes changes in coordination mode of Ru(II)/acylthiourea organometallic complexes with cytotoxicity against human lung tumor cell lines. *J. Inorg. Biochem.* **2018**, *186*, 147−156.
(47) Ngah, F. A.; Zakariah, E.; Fakhar, I.; Hassan, N.; Heng, L.; Yamin, B.; Hasbullah, S. A New Thiourea Compound as Potential Ionophore for Metal Ion Sensor. *Indones. J. Chem.* **2018**, *18*, 116−120.
(48) Yang, Z.; Huang, X.; Yao, X.; Ji, H. Thiourea modified hyper-crosslinked polystyrene resin for heavy metal ions removal from aqueous solutions. *J. Appl. Polym. Sci.* **2018**, *135*, No. 45568.
(49) Dewil, R.; Guo, H.-L.; Zhang, S.; North, C.; Zhang, M.; Meng, X.-x.; Gao, X.-L. Alkyl Thiourea Functionalised Silica for the Effective Removal of Heavy Metals from Acanthopanax senticosus Extract. *BioMed Res. Int.* **2020**, *2020*, No. 9860425.
(50) Gholami, L.; Rahimi, G.; Nezhad, A. K. J. Effect of thiourea-modified biochar on adsorption and fractionation of cadmium and lead in contaminated acidic soil. *Int. J. Phytorem.* **2020**, *22*, 468−481.
(51) Wang, Y.; Cui, X.; Wang, Y.; Shan, W.; Lou, Z.; Xiong, Y. A thiourea cross-linked three-dimensional graphene aerogel as a broad-spectrum adsorbent for dye and heavy metal ion removal. *New J. Chem.* **2020**, *44*, 16285−16293.

https://doi.org/10.1021/acs.inorgchem.1c01068
Inorg. Chem. 2021, 60, 11984−12000

(52) Stezowski, J. J.; Hoard, J. L. Heavy Metal Ionophores: Correlations Among Structural Parameters of Complexed Nonpeptide Polyamino Acids. *Isr. J. Chem.* **1984**, *24*, 323−334.
(53) Dabbagh-Bazarbachi, H.; Clergeaud, G.; Quesada, I. M.; Ortiz, M.; O'Sullivan, C. K.; Fernández-Larrea, J. B. Zinc Ionophore Activity of Quercetin and Epigallocatechin-gallate: From Hepa 1-6 Cells to a Liposome Model. *J. Agric. Food Chem.* **2014**, *62*, 8085−8093.
(54) Clergeaud, G.; Dabbagh-Bazarbachi, H.; Ortiz, M.; Fernández-Larrea, J. B.; O'Sullivan, C. K. A simple liposome assay for the screening of zinc ionophore activity of polyphenols. *Food Chem.* **2016**, *197*, 916−923.
(55) Koch, K. R. New chemistry with old ligands: N-alkyl- and N,N-dialkyl-N′-acyl(aroyl)thioureas in co-ordination, analytical and process chemistry of the platinum group metals. *Coord. Chem. Rev.* **2001**, *216−217*, 473−488.
(56) Saeed, A.; Mustafa, M. N.; ul Abideen, M. Z.; Shabir, G.; Erben, M. F.; Flörke, U. Current developments in chemistry, coordination, structure and biological aspects of 1-(acyl/aroyl)-3- (substituted)-thioureas: advances Continue ... *J. Sulfur Chem.* **2019**, *40*, 312−350.
(57) Noufele, C. N.; Pham, C. T.; Hagenbach, A.; Abram, U. Uranyl Complexes with Aroylbis(N,N-dialkylthioureas). *Inorg. Chem.* **2018**, *57*, 12255−12269.
(58) Alcamí, M.; González, A.; Mó, O.; Yáñez, M. Performance of density functional theory methods for the treatment of metal-ligand dications. *Chem. Phys. Lett.* **1999**, *307*, 244−252.
(59) Bertrán, J.; Rodríguez-Santiago, L.; Sodupe, M. The Different Nature of Bonding in Cu+-Glycine and Cu2+-Glycine. *J. Phys. Chem. B* **1999**, *103*, 2310−2317.
(60) Rulíšek, L.; Havlas, Z. Theoretical Studies of Metal Ion Selectivity. 1. DFT Calculations of Interaction Energies of Amino Acid Side Chains with Selected Transition Metal Ions (Co2+, Ni2+, Cu2+, Zn2+, Cd2+, and Hg2+). *J. Am. Chem. Soc.* **2000**, *122*, 10428−10439.
(61) Rulíšek, L.; Havlas, Z. Theoretical Studies of Metal Ion Selectivity.† 2. DFT Calculations of Complexation Energies of Selected Transition Metal Ions (Co2+, Ni2+, Cu2+, Zn2+, Cd2+, and Hg2+) in Metal-Binding Sites of Metalloproteins. *J. Phys. Chem. A* **2002**, *106*, 3855−3866.
(62) Lamsabhi, A. M.; Alcamí, M.; Mó, O.; Yáñez, M. Gas-Phase Reactivity of Uracil, 2-Thiouracil, 4-Thiouracil, and 2,4-Dithiouracil towards the Cu+ Cation: A DFT Study. *Chem. Phys. Chem.* **2003**, *4*, 1011−1016.
(63) Lamsabhi, A. M.; Alcamí, M.; Mó, O.; Yáñez, M.; Tortajada, J. Association of Cu2+ with Uracil and Its Thio Derivatives: A Theoretical Study. *ChemPhysChem* **2004**, *5*, 1871−1878.
(64) Schröder, D. Coulomb Explosions and Stability of Multiply Charged Ions in the Gas Phase. *Angew. Chem., Int. Ed.* **2004**, *43*, 1329−1331.
(65) Corral, I.; Mó, O.; Yáñez, M.; Radom, L. Why Are the Ca2+ and K+ Binding Energies of Formaldehyde and Ammonia Reversed with Respect to Their Proton Affinities? *J. Phys. Chem. A* **2005**, *109*, 6735−6742.
(66) Georgieva, I.; Trendafilova, N.; Rodríguez-Santiago, L.; Sodupe, M. Coordination Properties of the Oxime Analogue of Glycine to Cu(II). *J. Phys. Chem. A* **2005**, *109*, 5668−5676.
(67) Marino, T.; Toscano, M.; Russo, N.; Grand, A. Structural and Electronic Characterization of the Complexes Obtained by the Interaction between Bare and Hydrated First-Row Transition-Metal Ions (Mn2+, Fe2+, Co2+, Ni2+, Cu2+, Zn2+) and Glycine. *J. Phys. Chem. B* **2006**, *110*, 24666−24673.
(68) Trujillo, C.; Lamsabhi, A. M.; Mó, O.; Yáñez, M. The importance of the oxidative character of doubly charged metal cations in binding neutral bases. [Urea-M]2+ and [thiourea-M]2+ (M = Mg, Ca, Cu) complexes. *Phys. Chem. Chem. Phys.* **2008**, *10*, 3229−3235.
(69) Jang, S.; Ju Song, M.; Kim, H.; Choi, S.-S. Formation of metal complex ions from amino acid in the presence of Li+, Na+ and K+ by electrospray ionization: metal replacement of hydrogen in the ligands. *J. Mass Spectrom.* **2011**, *46*, 496−501.
(70) Burt, M. B.; Decker, S. G. A.; Fridgen, T. D. Water binding energies of [Pb(amino acid-H)H2O]+ complexes determined by blackbody infrared radiative dissociation. *Phys. Chem. Chem. Phys.* **2012**, *14*, 15118−15126.
(71) Hancock, R. D.; Bartolotti, L. J. A DFT analysis of the effect of chelate ring size on metal ion selectivity in complexes of polyamine ligands. *Polyhedron* **2013**, *52*, 284−293. SPecial Issue 100th Anniversary of the Award of the 1913 Nobel Prize in Chemistry to Alfred Werner: A Celebration.
(72) Montero-Campillo, M. M.; Lamsabhi, A. M.; Mó, O.; Yáñez, M. Alkyl mercury compounds: an assessment of DFT methods. *Theor. Chem. Acc.* **2013**, *132*, 1328.
(73) Aguilar-Galindo, F.; Montero-Campillo, M. M.; Yáñez, M.; Mó, O. On the stability of [Pb(Proline)]2+ complexes. Reconciling theory with experiment. *Chem. Phys. Lett.* **2014**, *598*, 91−95.
(74) Mehandzhiyski, A. Y.; Riccardi, E.; van Erp, T. S.; Koch, H.; Åstrand, P.-O.; Trinh, T. T.; Grimes, B. A. Density Functional Theory Study on the Interactions of Metal Ions with Long Chain Deprotonated Carboxylic Acids. *J. Phys. Chem. A* **2015**, *119*, 10195−10203.
(75) Tsaturyan, A. A.; Budnyk, A. P.; Ramalingan, C. DFT Study of the CNS Ligand Effect on the Geometry, Spin-State, and Absorption Spectrum in Ruthenium, Iron, and Cobalt Quaterpyridine Complexes. *ACS Omega* **2019**, *4*, 10991−11003.
(76) Mó, O.; Yáñez, M.; Total, A.; Tortajada, J.; Morizur, J. P. Structures and stabilities of [C2H5NAl]+ molecular ions: an ab initio molecular orbital study. *J. Phys. Chem. A* **1993**, *97*, 5553−5561.
(77) Peschke, M.; Blades, A. T.; Kebarle, P. Binding Energies for Doubly-Charged Ions M2+ = Mg2+, Ca2+ and Zn2+ with the Ligands L = H2O, Acetone and N-methylacetamide in Complexes M for n = 1 to 7 from Gas Phase Equilibria Determinations and Theoretical Calculations. *J. Am. Chem. Soc.* **2000**, *122*, 10440−10449.
(78) Alcamí, M.; Mó, O.; Yáñez, M. Computational chemistry: A useful (sometimes mandatory) tool in mass spectrometry studies. *Mass Spectrom. Rev.* **2001**, *20*, 195−245.
(79) Jaeger, T. D.; van Heijnsbergen, D.; Klippenstein, S. J.; von Helden, G.; Meijer, G.; Duncan, M. A. Vibrational Spectroscopy and Density Functional Theory of Transition-Metal Ion-Benzene and Dibenzene Complexes in the Gas Phase. *J. Am. Chem. Soc.* **2004**, *126*, 10981−10991.
(80) Guillaumont, S.; Tortajada, J.; Salpin, J.-Y.; Lamsabhi, A. M. Experimental and computational study of the gas-phase interactions between lead(II) ions and two pyrimidic nucleobases: Uracil and thymine. *Int. J. Mass Spectrom.* **2005**, *243*, 279−293.
(81) Corral, I.; Mó, O.; Yáñez, M.; Salpin, J.-Y.; Tortajada, J.; Moran, D.; Radom, L. An Experimental and Theoretical Investigation of Gas-Phase Reactions of Ca2+ with Glycine. *Chem. Eur. J.* **2006**, *12*, 6787−6796.
(82) Mó, O.; Yáñez, M.; Salpin, J.-Y.; Tortajada, J. Thermochemistry, bonding, and reactivity of Ni+ and Ni2+ in the gas phase. *Mass Spectrom. Rev.* **2007**, *26*, 474−516.
(83) Trujillo, C.; Mó, O.; Yáñez, M.; Salpin, J.-Y.; Tortajada, J. Gas-Phase Reactions Between Thiourea and Ca2+: New Evidence for the Formation of [Ca(NH3)]2+ and Other Doubly Charged Species. *ChemPhysChem* **2007**, *8*, 1330−1337.
(84) Belcastro, M.; Marino, T.; Russo, N.; Toscano, M. The role of glutathione in cadmium ion detoxification: Coordination modes and binding properties - A density functional study. *J. Inorg. Biochem.* **2009**, *103*, 50−57.
(85) Salpin, J.-Y.; Guillaumont, S.; Tortajada, J.; Al Lamsabhi, M. Gas-phase interactions between lead(II) ions and thiouracil nucleobases: A combined experimental and theoretical study. *J. Am. Soc. Mass Spectrom.* **2009**, *20*, 359−369.
(86) Hurtado, M.; Monte, M.; Lamsabhi, A. M.; Yáñez, M.; Mó, O.; Salpin, J.-Y. Modeling Interactions between an Amino Acid and a Metal Dication: Cysteine-Calcium(II) Reactions in the Gas Phase. *ChemPlusChem* **2013**, *78*, 1124−1133.
(87) Regulska, E.; Kalinowska, M.; Wojtulewski, S.; Korczak, A.; Sienkiewicz-Gromiuk, J.; Rzaczynska, Z.; Swislocka, R.; Lewandowski,

https://doi.org/10.1021/acs.inorgchem.1c01068
Inorg. Chem. 2021, 60, 11984−12000

W. Theoretical (in B3LYP/6-3111++G** level), spectroscopic (FT-IR, FT-Raman) and thermogravimetric studies of gentisic acid and sodium, copper(II) and cadmium(II) gentisates. *Spectrochim. Acta, Part A* **2014**, *132*, 713−725.
(88) Sanotra, S.; Gupta, R.; Gupta, U.; Khajuria, Y.; Sheikh, H. N. Synthesis, crystal structure, photoluminescence, and DFT studies of bis(1,10-phenanthroline)di(k2OO′ nitrato)cadmium(II) [Cd(phen)-2(NO3)2]. *Spectrochim. Acta, Part A* **2014**, *129*, 392−399.
(89) Power, B.; Haldys, V.; Salpin, J.-Y.; Fridgen, T. D. Structures of [M(Ura-H)(H2O)n]+ (M = Mg, Ca, Sr, Ba; n = 1-3) complexes in the gas phase by IRMPD spectroscopy and theoretical studies. *J. Mass Spectrom.* **2016**, *51*, 236−244.
(90) Power, B.; Rowe, S.; Fridgen, T. D. Ammoniated Complexes of Uracil and Transition Metal Ions: Structures of [M(Ura-H)(Ura)-(NH3)]+ by IRMPD Spectroscopy and Computational Methods (M = Fe, Co, Ni, Cu, Zn, Cd). *J. Phys. Chem. B* **2017**, *121*, 58−65.
(91) Butler, M.; Cabrera, G. M. A mass spectrometry and DFT study of pyrithione complexes with transition metals in the gas phase. *J. Mass Spectrom.* **2017**, *52*, 728−738.
(92) Pan, R.-K.; Wang, Y.; Song, J.-L.; Liu, S.-G. Two cadmium(II) complexes derived from bidentate bis(benzoimidazol-2-ylmethyl)-cyclohexane ligands: synthesis, crystal structures, spectroscopic and DFT calculations. *Chem. Pap.* **2018**, *72*, 2181−2191.
(93) Salpin, J.-Y.; Latrous, L.; Haldys, V.; Lamsabhi, A. M. Interactions of Dimethyltin(IV) with Uracil As Studied in the Gas Phase. *J. Phys. Chem. A* **2018**, *122*, 992−1003.
(94) Cheng, R.; Rose, V. E.; Power, B.; Fridgen, T. D. Self-assembled uracil complexes containing tautomeric uracils: an IRMPD spectroscopic and computation study of the structures of gaseous uracil$_n$Ca2+ (n = 4, 5, or 6) complexes. *Phys. Chem. Chem. Phys.* **2018**, *20*, 572−580.
(95) Power, B.; Haldys, V.; Salpin, J.-Y.; Fridgen, T. D. Structures of [M(Ura-H)(Ura)]+ and [M(Ura-H)(H2O)n]+ (M=Cu, Zn, Pb; n=1−3) complexes in the gas phase by IRMPD spectroscopy in the fingerprint region and theoretical studies. *Int. J. Mass Spectrom.* **2018**, *429*, 56−65. Terry B. McMahon 70th Birthday Special Issue: Mass Spectrometry and its Application to the Physical Chemistry of Gaseous Ions.
(96) Salpin, J.-Y.; Haldys, V.; Latrous, L.; Guillemin, J.-C.; Tortajada, J.; Léon, E.; Mó, O.; Yáñez, M.; Montero-Campillo, M. M. Alkylation of uracil and thymine in the gas phase through interaction with alkylmercury compounds. *Int. J. Mass Spectrom.* **2019**, *436*, 153−165.
(97) Lamsabhi, A. M.; Mó, O.; Yáñez, M.; Salpin, J.-Y. Combined Experimental and Theoretical Survey of the Gas-Phase Reactions of Serine−Ca2+ Adducts. *J. Phys. Chem. A* **2019**, *123*, 6241−6250.
(98) Frisch, M. J.; et al. *Gaussian 09*, revision E.01; Gaussian Inc.: Wallingford, CT, 2009.
(99) Becke, A. D. Density-functional thermochemistry. III. The role of exact exchange. *J. Chem. Phys.* **1993**, *98*, 5648−5652.
(100) Lee, C.; Yang, W.; Parr, R. G. Development of the Colle-Salvetti correlation-energy formula into a functional of the electron density. *Phys. Rev. B* **1988**, *37*, 785−789.
(101) Ditchfield, R.; Hehre, W. J.; Pople, J. A. Self-Consistent Molecular-Orbital Methods. IX. An Extended Gaussian-Type Basis for Molecular-Orbital Studies of Organic Molecules. *J. Chem. Phys.* **1971**, *54*, 724−728.
(102) Dunning, T. H.; Ha, P. J. In *Modern Theoretical Chemistry*; Schaefer, H. F., III, Ed.; Plenum: New York, 1977; Vol. 3; pp 1−28.
(103) Iyengar, S. S.; Schlegel, H. B.; Millam, J. M.; A Voth, G.; Scuseria, G. E.; Frisch, M. J. Ab initio molecular dynamics: Propagating the density matrix with Gaussian orbitals. II. Generalizations based on mass-weighting, idempotency, energy conservation and choice of initial conditions. *J. Chem. Phys.* **2001**, *115*, 10291−10302.
(104) Schlegel, H. B.; Millam, J. M.; Iyengar, S. S.; Voth, G. A.; Daniels, A. D.; Scuseria, G. E.; Frisch, M. J. Ab initio molecular dynamics: Propagating the density matrix with Gaussian orbitals. *J. Chem. Phys.* **2001**, *114*, 9758−9763.
(105) Schlegel, H. B.; Iyengar, S. S.; Li, X.; Millam, J. M.; Voth, G. A.; Scuseria, G. E.; Frisch, M. J. Ab initio molecular dynamics: Propagating the density matrix with Gaussian orbitals. III. Comparison with Born-Oppenheimer dynamics. *J. Chem. Phys.* **2002**, *117*, 8694−8704.
(106) Bader, R. *Atoms in Molecules: A Quantum Theory*; Oxford University Press: Oxford, 1990.
(107) Keith, T. A. *AIMAll*, version 19.10.12, TK Gristmill Software. Overland Park KS, aim.tkgristmill.com, 2019.
(108) Schiessl, W. C.; Summa, N. K.; Weber, C. F.; Gubo, S.; Dücker-Benfer, C.; Puchta, R.; van Eikema Hommes, N. J. R.; van Eldik, R. Experimental and Theoretical Approaches to the Protonation of Thiourea: A Convenient Nucleophile in Coordination Chemistry Revisited. *Z. Anorg. Allg. Chem* **2005**, *631*, 2812−2819.
(109) Mertschenk, B.; Knott, A.; Bauer, W. *Ullmann's Encyclopedia of Industrial Chemistry*; American Cancer Society, 2013; pp 1−15.
(110) Patai, S. *The Chemistry of the Thiol Group*; Wiley, 1974.
(111) Rostkowska, H.; Lapinski, L.; Khvorostov, A.; Nowak, M. J. Proton-Transfer Processes in Thiourea: UV Induced Thione → Thiol Reaction and Ground State Thiol → Thione Tunneling. *J. Phys. Chem. A* **2003**, *107*, 6373−6380.
(112) Isab, A. A.; Wazeer, M. I. Complexation of Zn (II), Cd (II) and Hg (II) with thiourea and selenourea: A 1H, 13C, 15N, 77Se and 113Cd solution and solid-state NMR study. *J. Coord. Chem.* **2005**, *58*, 529−537.
(113) Khaorapapong, N. In situ complexation of thiourea in the interlayer space of copper(II)-montmorillonite. *Appl. Clay Sci.* **2010**, *50*, 414−417.
(114) Cremer, D.; Kraka, E. Chemical Bonds without Bonding Electron Density−Does the Difference Electron-Density Analysis Suffice for a Description of the Chemical Bond? *Angew. Chem., Int. Ed.* **1984**, *23*, 627−628.
(115) Espinosa, E.; Alkorta, I.; Elguero, J.; Molins, E. From weak to strong interactions: A comprehensive analysis of the topological and energetic properties of the electron density distribution involving X-H···F-Y systems. *J. Chem. Phys.* **2002**, *117*, 5529−5542.
(116) Zabardasti, A.; Afrouzi, H.; Kakanejadifard, A.; Jamshidi, Z. The S···P noncovalent interaction: diverse chalcogen bonds. *J. Sulfur Chem.* **2017**, *38*, 249−263.
(117) Mohammadi, M.; Khanmohammadi, A. Molecular structure, QTAIM and bonding character of cation-π interactions of mono-and divalent metal cations (Li+, Na+, K+, Be 2+, Mg 2+ and Ca 2+) with drug of acetaminophen. *Theor. Chem. Acc.* **2019**, *138*, No. 101.
(118) da Costa, L. M.; de Mesquita Carneiro, J. W.; Romeiro, G. A.; Paes, L. W. C. Interaction between alkaline earth cations and oxo-ligands. DFT study of the affinity of the Ca2+ cation for carbonyl ligands. *J. Mol. Model.* **2011**, *17*, 243−249.
(119) da Costa, L. M.; Stoyanov, S. R.; Carneiro, J. W. dM. Interaction between alkaline earth cations and oxo ligands: a DFT study of the affinity of Mg 2+ for carbonyl ligands. *J. Mol. Model.* **2012**, *18*, 4389−4396.
(120) Trujillo, C.; Gámez, J. A. Kinetical and thermodynamical analysis of the reactivity of thiourea by association to Ca2+. *Comput. Theor. Chem.* **2015**, *1052*, 68−72.
(121) Corongiu, G.; Clementi, E. Study of the structure of molecular complexes. XVI. Doubly charged cations interacting with water. *J. Chem. Phys.* **1978**, *69*, 4885−4887.
(122) *CRC Handbook of Chemistry and Physics*; 88th ed.; Lide, D. R.CRC Press: Boca Raton, FL, 2008; Vol. *130*, pp 382.
(123) El-Nahas, A. M.; El-Demerdash, S. H.; El-Shereefy, E.-S. E. Quantum chemical calculations on the structure and stability of Mg2+XH3OH complexes in the gas phase (X=C, Si, and Ge). *Int. J. Mass Spectrom.* **2007**, *263*, 267−275.
(124) Brea, O.; Yáñez, M.; Mó, O.; Lamsabhi, A. M. On the stability of [(uracil)2-Cu]2+ complexes in the gas phase. Different pathways for the formation of [(uracil-H)(uracil)-Cu]+ monocations. *Org. Biomol. Chem.* **2013**, *11*, 3862−3870.
(125) Süleymanoğlu, N.; Ustabaş, R.; Şahin Direkel; Alpaslan, Y. B.; Ünver, Y. 1,2,4-triazole derivative with Schiff base; thiol-thione

https://doi.org/10.1021/acs.inorgchem.1c01068
Inorg. Chem. 2021, 60, 11984−12000

tautomerism, DFT study and antileishmanial activity. *J. Mol. Struct.* **2017**, *1150*, 82−87.
(126) Bagheri, S.; Roohi, H. Proton-Transfer Mechanism in 2-Thioxoimidazolidin-4-one: A Competition between Keto/Enol and Thione/Thiol Tautomerism Reactions. *Bull. Chem. Soc. Jpn.* **2009**, *82*, 446−452.
(127) Soliman, S. M.; Hagar, M.; Ibid, F.; El Ashry, E. S. H. Experimental and theoretical spectroscopic studies, HOMO-LUMO, NBO analyses and thione-thiol tautomerism of a new hybrid of 1,3,4-oxadiazole-thione with quinazolin-4-one. *Spectrochim. Acta, Part A* **2015**, *145*, 270−279.
(128) Alabugin, I. V.; dos Passos Gomes, G.; Abdo, M. A. Hyperconjugation. *Wiley Interdiscip. Rev.: Comput. Mol. Sci.* **2019**, *9*, No. e1389.
(129) Contreras Aguilar, E.; Echeverría, G.; Piro, O.; Ulic, S.; Jios, J.; Tuttolomondo, M.; Molina, R.; Arena, M. Acyl thiourea derivatives: A study of crystallographic, bonding, biological and spectral properties. *Chem. Phys. Lett.* **2019**, *715*, 64−71.
(130) Saeed, A.; Khurshid, A.; Bolte, M.; Fantoni, A. C.; Erben, M. F. Intra- and intermolecular hydrogen bonding and conformation in 1-acyl thioureas: An experimental and theoretical approach on 1-(2-chlorobenzoyl)thiourea. *Spectrochim. Acta, Part A* **2015**, *143*, 59−66.
(131) Ni, J.; Xu, G.; Dai, W.; Zhao, Y.-L.; Ni, Y. Hyperconjugation promoted by hydrogen bonding between His98/His241 and a carboxyl group contributes to tyrosine decarboxylase catalysis. *Catal. Sci. Technol.* **2019**, *9*, 6222−6226.
(132) Muthuraja, P.; Beaula, T. J.; Sethuram, M.; Jothy, V. B.; Dhandapani, M. Hydrogen bonding interactions on 1H-1,2,3-triazole based crystals: Featuring experimental and theoretical analysis. *Curr. Appl. Phys.* **2018**, *18*, 774−784.
(133) Imani, Z.; Mundlapati, V. R.; Goldsztejn, G.; Brenner, V.; Gloaguen, E.; Guillot, R.; Baltaze, J.-P.; Le Barbu-Debus, K.; Robin, S.; Zehnacker, A.; Mons, M.; Aitken, D. J. Conformation control through concurrent N-H···S and N-H···O=C hydrogen bonding and hyperconjugation effects. *Chem. Sci.* **2020**, *11*, 9191−9197.
(134) Banerjee, P.; Chakraborty, T. Correlation of νOH Spectral Shifts of Phenol−Benzene O-H···π Hydrogen-Bonded Complexes with Donor's Acidity: A Combined Matrix Isolation, Infrared Spectroscopy, and Quantum Chemistry Study. *J. Phys. Chem. A* **2014**, *118*, 7074−7084.
(135) Bryantsev, V. S.; Hay, B. P. Conformational Preferences and Internal Rotation in Alkyl- and Phenyl-Substituted Thiourea Derivatives. *J. Phys. Chem. A* **2006**, *110*, 4678−4688.
(136) Ocola, E. J.; Laane, J. Theoretical investigation of intramolecular π-type hydrogen bonding and internal rotation of 2-cyclopropen-1-ol, 2-cyclopropen-1-thiol and 2-cyclopropen-1-amine. *Mol. Phys.* **2019**, *117*, 1404−1412.
(137) Wang, D.; Chopra, P.; Wategaonkar, S.; Fujii, A. Electronic and Infrared Spectroscopy of Benzene-(H2S)n (n = 1 and 2): The Prototype of the SH-π Interaction. *J. Phys. Chem. A* **2019**, *123*, 7255−7260.
(138) Jian, J.; Poater, J.; Hammink, R.; Tinnemans, P.; McKenzie, C. J.; Bickelhaupt, F. M.; Mecinović, J. Through-Space Polar-π Interactions in 2,6-Diarylthiophenols. *ChemPhysChem* **2020**, *21*, 1092−1100.
(139) Nossa González, D. L.; Saeed, A.; Shabir, G.; Florke, U.; Erben, M. F. Conformational and crystal structure of acyl thiourea compounds: The case of the simple (2,2-dimethyl-propionyl) thiourea derivative. *J. Mol. Struct.* **2020**, *1215*, No. 128227.
(140) Echeverría, J.; Cirera, J.; Alvarez, S. Mercurophilic interactions: a theoretical study on the importance of ligands. *Phys. Chem. Chem. Phys.* **2017**, *19*, 11645−11654.
(141) Bensch, W.; Schuster, M. Komplexierung von Gold mit N,N-Dialkyl-N′-benzoythioharnstoffen: Die Kristallstruktur von N,N-Diethyl-N′-benzoylformamidin tetrachloroaurat (III). *Z. Anorg. Allg. Chem* **1992**, *611*, 95−98.
(142) Morell, C.; Gázquez, J. L.; Vela, A.; Guégan, F.; Chermette, H. Revisiting electroaccepting and electrodonating powers: proposals for local electrophilicity and local nucleophilicity descriptors. *Phys. Chem. Chem. Phys.* **2014**, *16*, 26832−26842.
(143) Ayers, P. W. An elementary derivation of the hard/soft-acid/base principle. *J. Chem. Phys.* **2005**, *122*, No. 141102.
(144) Ayers, P. W.; Parr, R. G.; Pearson, R. G. Elucidating the hard/soft acid/base principle: A perspective based on half-reactions. *J. Chem. Phys.* **2006**, *124*, No. 194107.
(145) Cairo, R. R.; Stevens, A. M. P.; de Oliveira, T. D.; Batista, A. A.; Castellano, E. E.; Duque, J.; Soria, D. B.; Fantoni, A. C.; Corrêa, R. S.; Erben, M. F. Understanding the conformational changes and molecular structure of furoyl thioureas upon substitution. *Spectrochim. Acta, Part A* **2017**, *176*, 8−17.
(146) Estévez-Hernández, O.; Duque, J.; Rodríguez-Hernández, J.; Reguera, E. Dinuclear and polymeric Hg(II) complexes with 1-(2-furoyl)thiourea derivatives: Their crystal structure and related properties. *Polyhedron* **2015**, *97*, 148−156.
(147) Li, X.; Sun, L.; Zhang, Q.; Li, S.; Wang, Y.; Wei, D.; Zhang, W.; Lan, Y. Mechanism and Substituent Effects of Benzene Arylation via a Phenyl Cation Strategy: A Density Functional Theory Study. *Chem. Cat. Chem.* **2019**, *11*, 5068−5076.
(148) Nam, P.-C.; Nguyen, M. T.; Chandra, A. K. Methyl and Phenyl Substitution Effects on the Proton Affinities of Hydrides of First and Second Row Elements and Substituent Effects on the Proton Affinities of Ring Carbons in Benzene: A DFT Study. *J. Phys. Chem. A* **2006**, *110*, 4509−4515.
(149) Saeed, A.; Flörke, U.; Erben, M. F. A review on the chemistry, coordination, structure and biological properties of 1-(acyl/aroyl)-3-(substituted) thioureas. *J. Sulfur Chem.* **2014**, *35*, 318−355.
(150) Biswal, H. S.; Wategaonkar, S. OH···X (X = O, S) hydrogen bonding in thetrahydrofuran and tetrahydrothiophene. *J. Chem. Phys.* **2011**, *135*, No. 134306.
(151) Domagała, M.; Grabowski, S. J. CH···N and CH···S Hydrogen Bonds Influence of Hybridization on Their Strength. *J. Phys. Chem. A* **2005**, *109*, 5683−5688.
(152) Pérez, H.; Ramos, R.; Plutín, A. M.; Mocelo, R.; Erben, M. F.; Castellano, E. E.; Batista, A. A. A Mixed Ligand Platinum(II) Complex: Spectral Analysis, Crystal Structure, Steric Demand of the Ligand, and Bioactivity of cis-[Pt(PPh3)2(L1-O,S)]PF6 (L1-O,S = N,N-Morpholine-N′-benzoylthiourea). *Eur. J. Inorg. Chem.* **2019**, *2019*, 2583−2590.
(153) Ferreirós-Martínez, R.; Esteban-Gómez, D.; Platas-Iglesias, C.; de Blas, A.; Rodríguez-Blas, T. Selective Chelation of Cd(II) and Pb(II) versus Ca(II) and Zn(II) by Using Octadentate Ligands Containing Pyridinecarboxylate and Pyridyl Pendants. *Inorg. Chem.* **2009**, *48*, 10976−10987.
(154) Kaviani, S.; Shahab, S.; Sheikhi, M.; Ahmadianarog, M. DFT study on the selective complexation of meso-2,3-dimercaptosuccinic acid with toxic metal ions (Cd2+, Hg2+ and Pb2+) for pharmaceutical and biological applications. *J. Mol. Struct.* **2019**, *1176*, 901−907.
(155) Seth, S. K.; Bauzá, A.; Mahmoudi, G.; Stilinović, V.; López-Torres, E.; Zaragoza, G.; Keramidas, A. D.; Frontera, A. On the importance of Pb···X (X = O, N, S, Br) tetrel bonding interactions in a series of tetra- and hexa-coordinated Pb(II) compounds. *CrystEngComm* **2018**, *20*, 5033−5044.
(156) Shiraishi, Y.; Sumiya, S.; Hirai, T. A coumarin−thiourea conjugate as a fluorescent probe for Hg(ii) in aqueous media with a broad pH range 2-12. *Org. Biomol. Chem.* **2010**, *8*, 1310−1314.
(157) Zhao, Y.; Lin, Z.; He, C.; Wu, H.; Duan, C. A "Turn-On" Fluorescent Sensor for Selective Hg(II) Detection in Aqueous Media Based on Metal-Induced Dye Formation. *Inorg. Chem.* **2006**, *45*, 10013−10015.
(158) Hu, Y.; Xin, X.; Wan, B. Cyclization reactions of propargylic amides: mild access to N-heterocycles. *Tetrahedron Lett.* **2015**, *56*, 32−52.
(159) Malaganvi, S. S.; Tonannavar Yenagi, J.; Tonannavar, J. Experimental, DFT dimeric modeling and AIM study of H-bond-mediated composite vibrational structure of Chelidonic acid. *Heliyon* **2019**, *5*, No. e01586.

https://doi.org/10.1021/acs.inorgchem.1c01068
Inorg. Chem. 2021, 60, 11984−12000